The National Center for Hypersonic Laminar-Turbulent Transition Research



Numerical Investigation of High Speed Boundary Layer Stabilization Through Porous Walls*

Christoph Hader
The University of Arizona

Intern at Applied Modeling & Simulation Branch,
NASA Ames Research Center
Mentor: Cetin Kiris

* C. Hader, C. Brehm, H.F. Fasel, “Numerical Investigation of transition delay for various controlled breakdown scenarios in a Mach 6 Boundary Layer using porous walls”, AIAA 2014-2500

http://hypersonics.tamu.edu/

Outline



Introduction/Motivation

Governing Equations and Numerical Methods

Base Flow and Disturbance Generation

Linear Regime

Nonlinear Regime

Summary

Introduction/Motivation

"The location of transition is of critical importance in the design of [...] hypersonic vehicles as both the aerodynamic heating and skin friction are higher in transitional and turbulent flows compared to laminar flow.

[...] A delay of the transition from a laminar-to-turbulent state will facilitate the optimal design of hypersonic vehicles [...]

Chokani et al. (2005)

HIFiRE



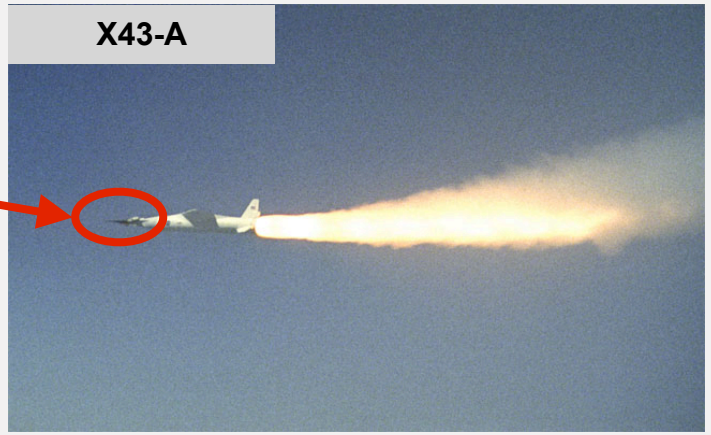
http://www.nasa.gov/images/content/648007main_hifire01-610x800.jpg

X43-A



http://en.wikipedia.org/wiki/NASA_X-43#mediaviewer/File:X43a2_nasa_scramjet.jpg

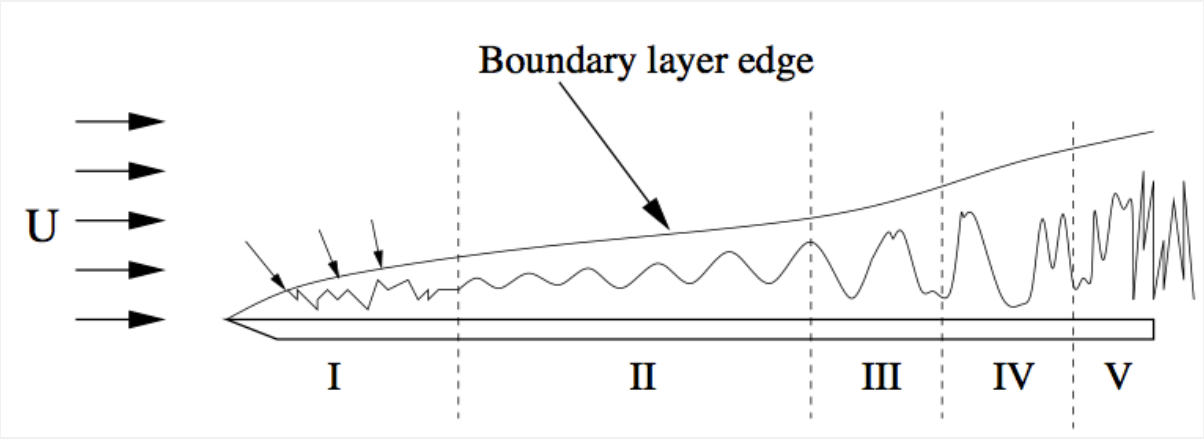
X43-A



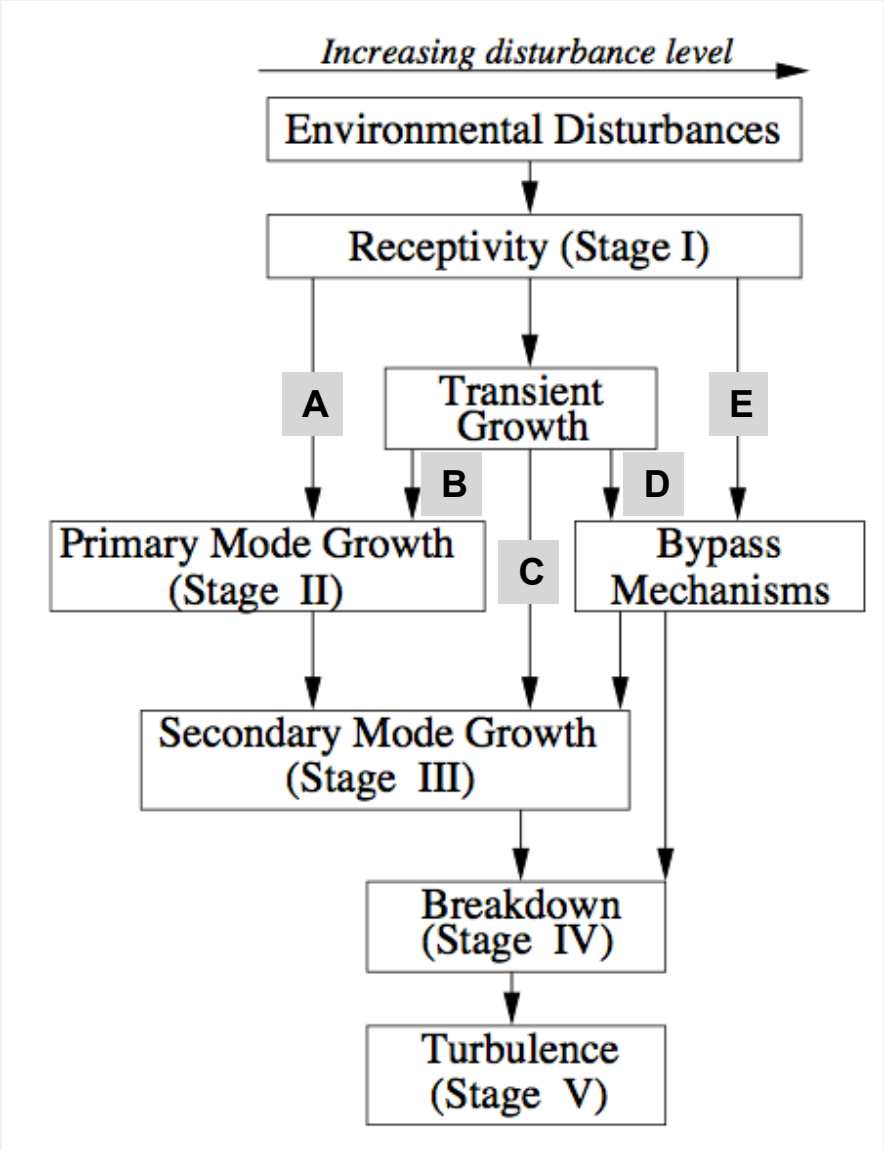
http://en.wikipedia.org/wiki/NASA_X-43#mediaviewer/File:X-43A.jpg

Introduction/Motivation

- Various paths to transition
- Low disturbance environment, no surface roughness ⇒ path A



Schematic of transition stages. (*Terwilliger (2011)*)

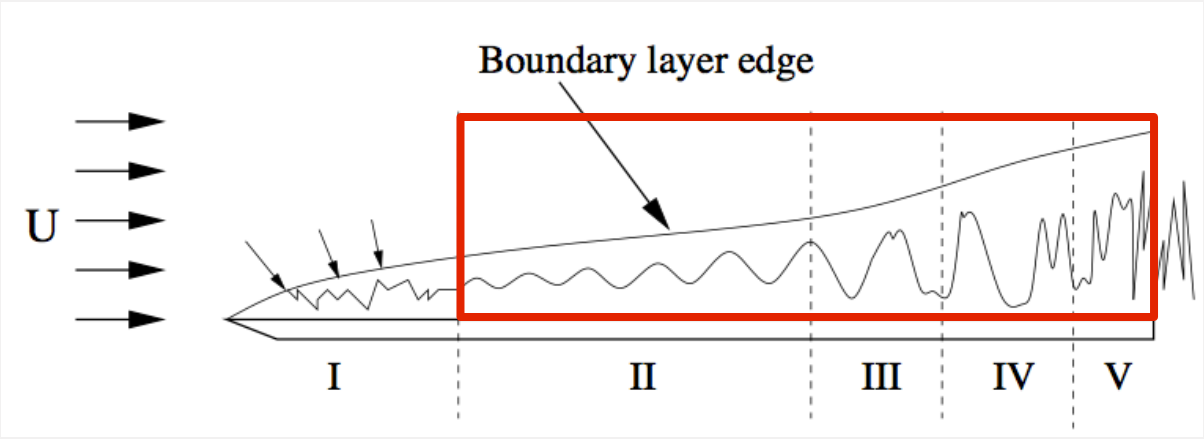


Paths to transition (*Terwilliger (2011)*)

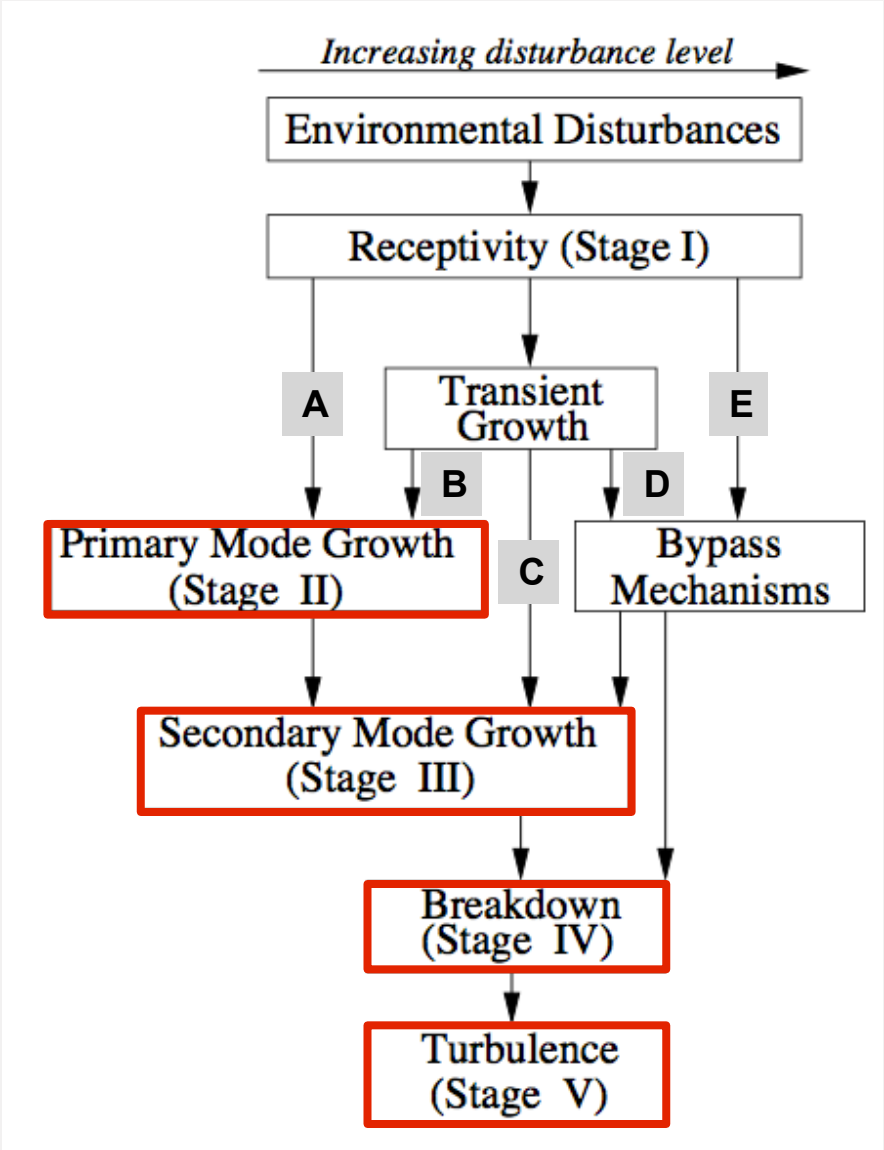
Introduction/Motivation

- Various paths to transition
- Low disturbance environment, no surface roughness ⇒ path A

Focus here on parts of path A



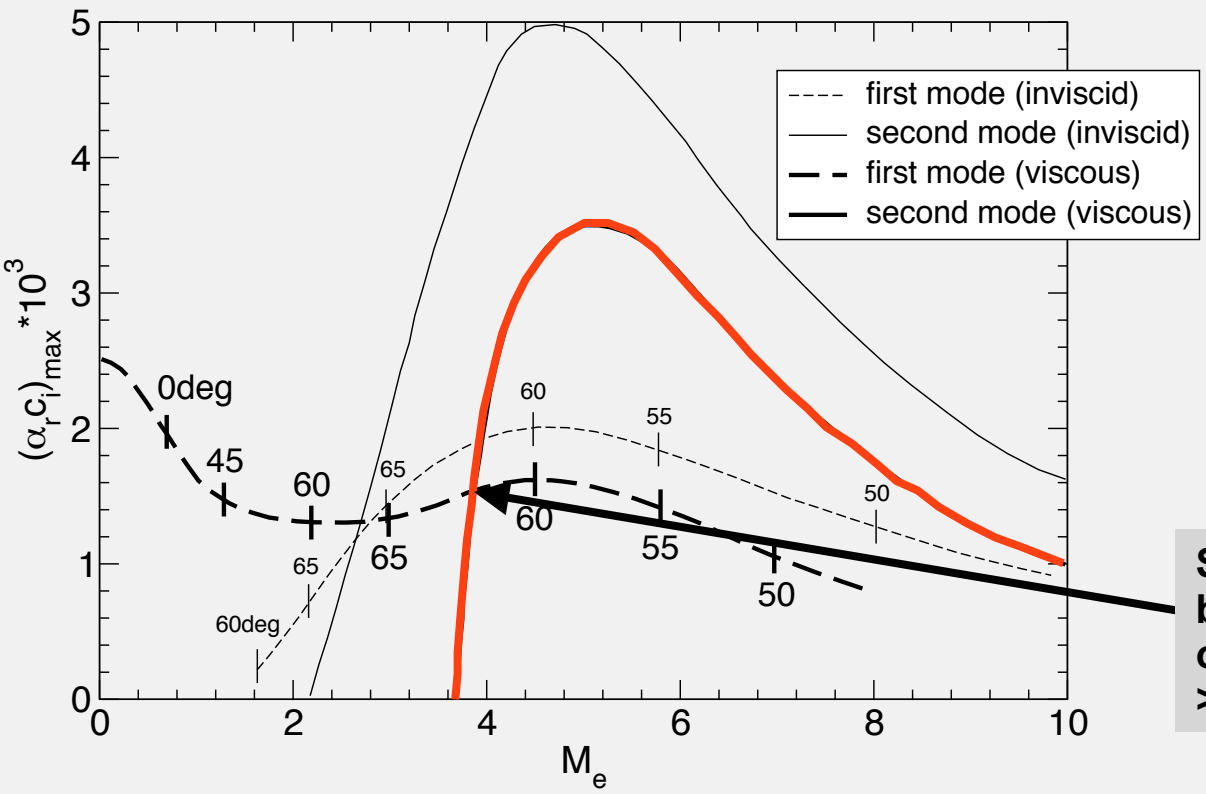
Schematic of transition stages. (*Terwilliger (2011)*)



Paths to transition (*Terwilliger (2011)*)

Introduction/Motivation

- Sharp leading edges, relatively low angles of attack results in high Mach numbers in the Boundary Layer
- Most amplified waves: **2D second mode waves** (Compressible LST, *Mack (1969)*)

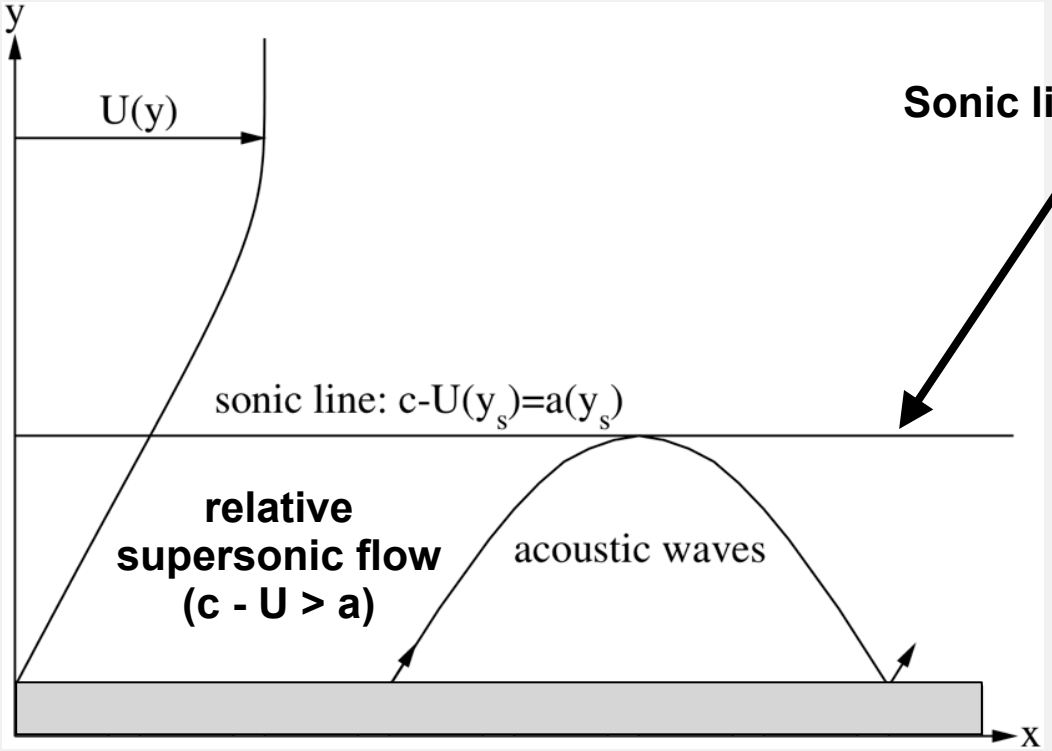


Second mode becomes dominant over first mode for M > 4

Maximum temporal amplification rate vs edge Mach number (*Mack (1969)*)

Introduction/Motivation

- Second mode waves are acoustic waves in ultrasonic frequency spectrum (confirmed by experiments: *Stetson et al. (1983)*)
- Relative supersonic flow region in Boundary Layer
- Trapped acoustic waves (*Fedorov et al. (2001)*)



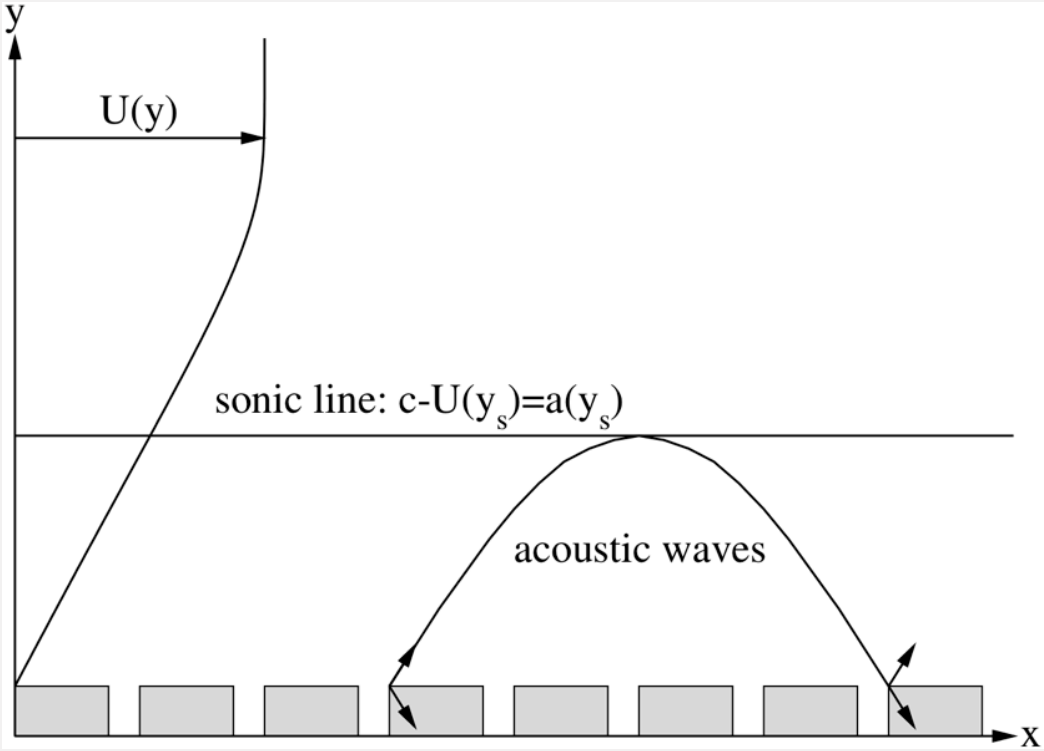
Sonic line acts like a waveguide

c = disturbance phase speed
a = local speed of sound
U = mean flow velocity

Disturbance wave schematic (*Fedorov et al. 2001*)

Introduction/Motivation

Idea: Stabilization of second mode waves through absorbing acoustic energy of trapped acoustic waves (Fedorov et al. 2001)



Disturbance wave schematic (*Fedorov et al. 2001*)

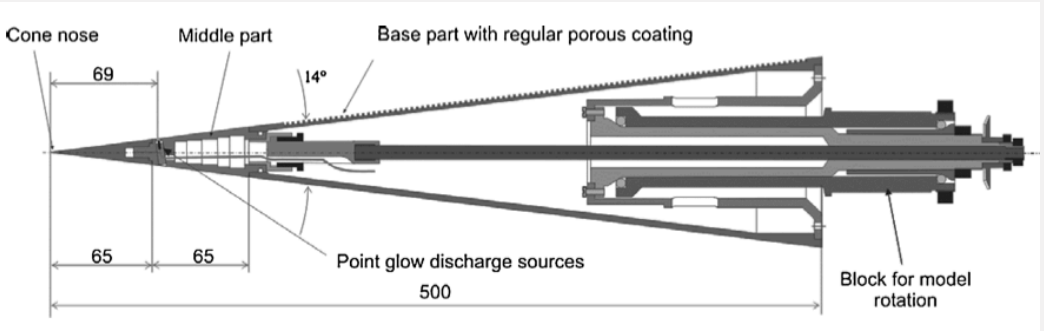
Related Research



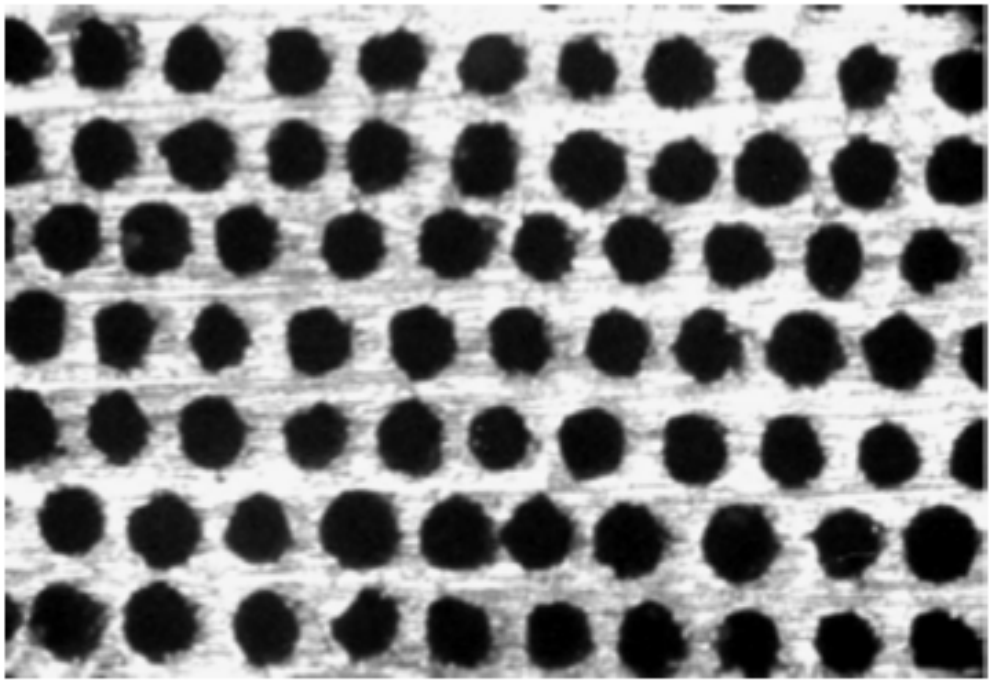
- Many numerical studies have been conducted for the linear stability regime to confirm the stabilizing behavior of porous walls (*Fedorov (2010), Bres et al. (2008/2009), Sandham et al. (2009), Wartemann et al. (2010)*, ...)
- Boundary Conditions employed to account for presence of porous wall
- Few numerical studies have been conducted of porous walls for the nonlinear stability regime where the pores are resolved (*de Tullio et al. (2010)*)
- Experiments showed potential of porous walls to stabilize BL (*Rasheed et al. (2002), Chokani et al. (2005), Fedorov et al. (2006)*)
- Fair agreement between experiments and numerical results

Intermediate Summary

- Passive laminar flow control techniques important for design optimization
- Stabilization of dominant second mode through porous walls
- Interest in effect of porous walls on nonlinear regime



Schematic of sharp cone model (*Fedorov et al. 2005*)



Micrograph of perforated sheet (*Fedorov et al. 2005*)

Outline



Introduction/Motivation

Governing Equations and Numerical Methods

Base Flow and Disturbance Generation

Linear Regime

Nonlinear Regime

Summary

Governing Equations/ Numerical Methods



Equations and assumptions:

- Solution of the compressible Navier Stokes Equations

$$\frac{\partial \boldsymbol{U}}{\partial t} + \frac{\partial \left(\boldsymbol{E_c} + \boldsymbol{E_d}\right)}{\partial x} + \frac{\partial \left(\boldsymbol{F_c} + \boldsymbol{F_d}\right)}{\partial y} + \frac{\partial \left(\boldsymbol{G_c} + \boldsymbol{G_d}\right)}{\partial z} + \boldsymbol{F_{force}} = 0$$

- perfect gas (Pr = 0.72, γ = 1.4, c_p = const.)
- Sutherland's law to compute viscosity

$$\mu = T^{\frac{3}{2}} \frac{1 + \frac{C}{T_\infty^*}}{T + \frac{C}{T_\infty^*}}$$

Numerical Scheme:

- Convective terms: Upwind biased centered finite differences, $O(\Delta x^9)$ *(Zhong (1998))*, van Leer flux splitting scheme
- Viscous terms: Centered finite differences, $O(\Delta x^8)$
- Time integration: Runge-Kutta, $O(\Delta t^4)$

Governing Equations/ Numerical Methods



Temporal approach for disturbance simulations:

- many pores per disturbance wavelength have to be resolved ⇒ high resolution requirements for spatial DNS
- traveling wave ansatz: $\phi'(x,y,t) = \hat{\phi}(y)e^{i(\alpha x - \omega t)}$

Temporal Model

<u>assumptions:</u>
- α is real
- ω is complex

→ disturbance grows in time

$$\phi'(x,y,t) = \hat{\phi}(y)e^{(i(\alpha x - \omega_r t))}e^{\omega_i t}$$

- amplification for $\omega_i > 0$, decay for $\omega_i < 0$
- non-parallel effects through boundary layer growth not captured (parallel Base Flow enforced)

Spatial Model

<u>assumptions:</u>
- α is complex
- ω is real

→ disturbance grows in space

$$\phi'(x,y,t) = \hat{\phi}(y)e^{(i(\alpha_r x - \omega_r t))}e^{-\alpha_i x}$$

- amplification for $\alpha_i < 0$, decay for $\alpha_i > 0$
- most realistic case
- computationally very expensive

Governing Equations/ Numerical Methods

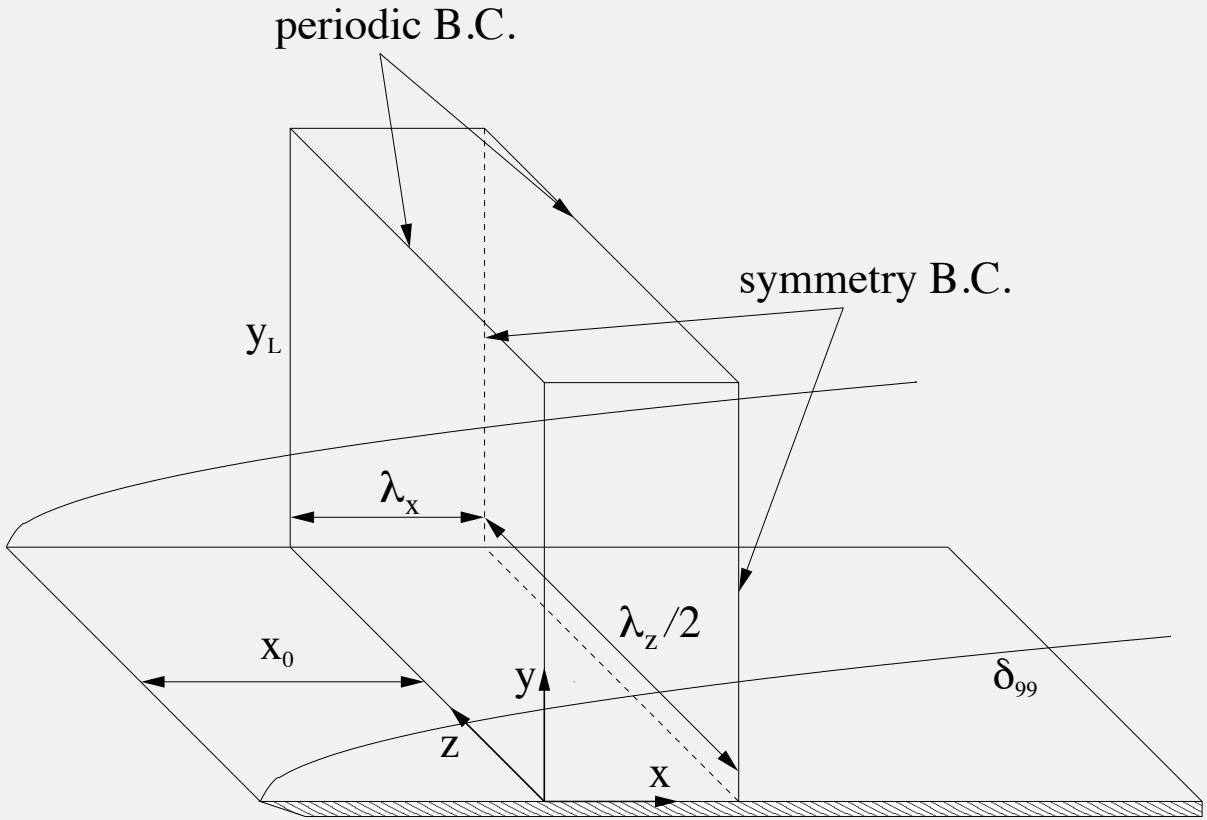
Boundary Conditions:

- periodic in streamwise direction
- symmetry in spanwise direction
- no slip, adiabatic wall
- exponential decay at upper boundary

Base Flow forcing:

- suppress boundary layer growth in streamwise direction

$$\mathbf{F_{force}} = -\frac{\partial\left(\mathbf{F_c} + \mathbf{F_d}\right)}{\partial y}$$



Schematic of computational domain for temporal approach

Porous wall:

- physically resolved with higher-order Immersed Boundary Method (*Brehm & Fasel, JCP, 2013 Vol. 242, Brehm et al. AIAA 2014-2093, Brehm et al. AIAA 2014-2093*)

Outline



Introduction/Motivation

Governing Equations and Numerical Methods

Base Flow and Disturbance Generation

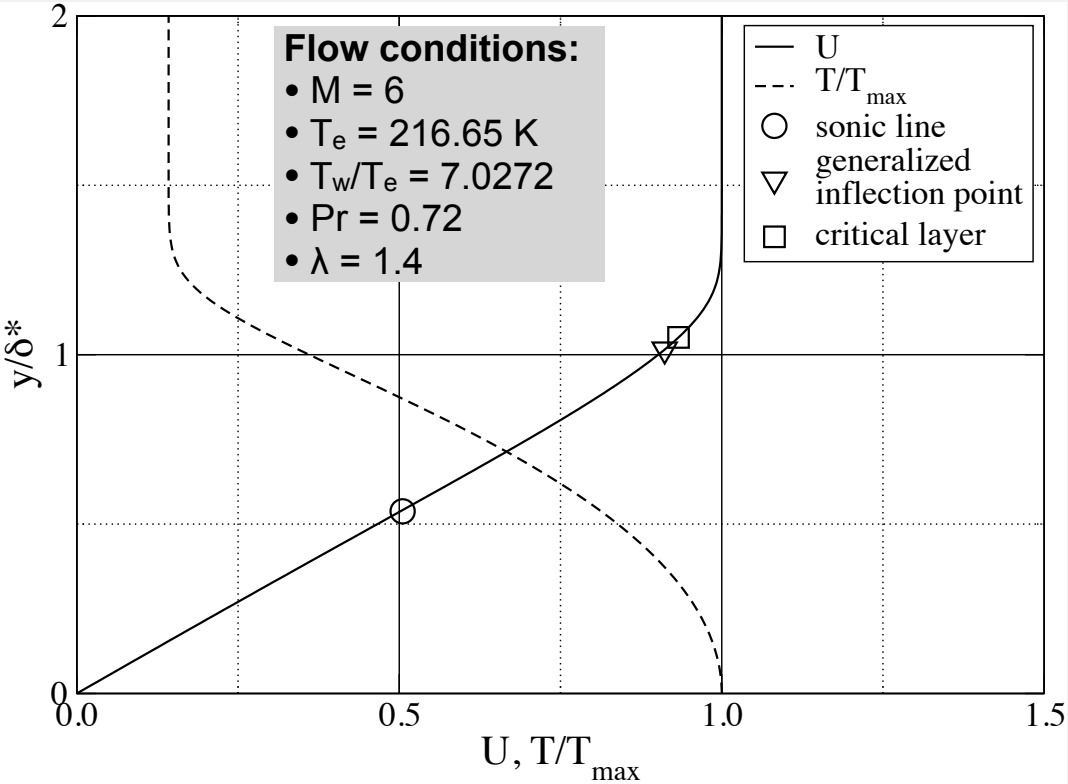
Linear Regime

Nonlinear Regime

Summary

Base Flow and Disturbance Generation

- **Initial condition:** similarity solution of compressible BL equations
- adiabatic wall
- **Flow conditions:** consistent with *Sandham et al. (2009), Wartemann et al. (2010), deTullio et al. (2010) and Fedorov et al.(2011)*
- reference length scale: displacement thickness δ*
- Re_{δ^*} = 20000
- x_0/δ^* = 114.54
- **Disturbance forcing:** volume force in y-momentum equation



Base Flow profiles

$$\mathrm{RHS}_{\text{y-momentum}} = \mathrm{RHS}_{\text{y-momentum}} + f(x, y, z, t), \quad \text{for} \quad 0 \le t \le T$$

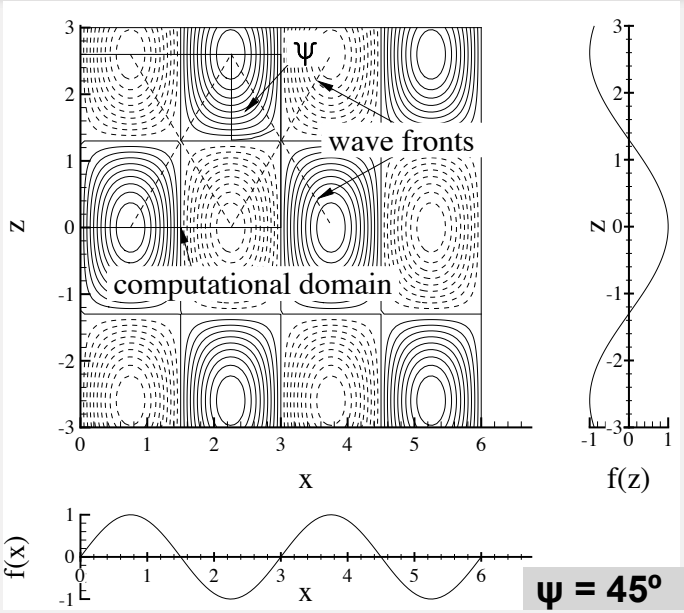
Base Flow and Disturbance Generation

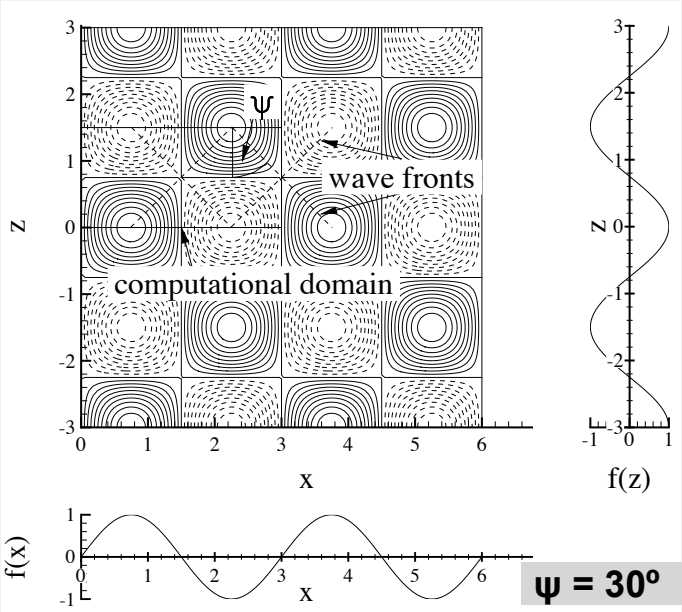
- forcing function

$$f(x,y,z,t) = \cos(\omega_r t)\, e^{-\left(\frac{y-y_{vf}}{\sigma_y}\right)^2} \sum_{i=1}^{n_{forcing}} A_{forcing,i} \sin(m_{x,i}\alpha_r x) \cos\left(m_{z,i}\frac{\beta_r}{2} z\right)$$

- ω_r: frequency
- $\alpha_r = 2\pi/\lambda_x$: streamwise wavenumber
- $\beta_r = 2\pi/\lambda_z$: spanwise wavenumber
- fundamental wavenumber defined by domain size (L_x, L_z)
- $\alpha_{fund} = 2\pi/L_x$; $\beta_{fund} = 2\pi/L_z$
- wave angle is controlled by extent of computational domain

$$\psi = \arctan\left(\frac{\beta_r}{\alpha_r}\right)$$





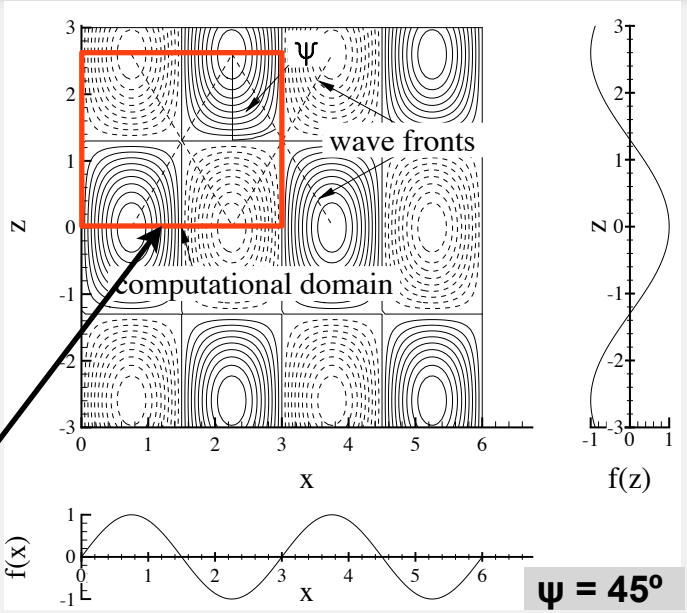
Base Flow and Disturbance Generation

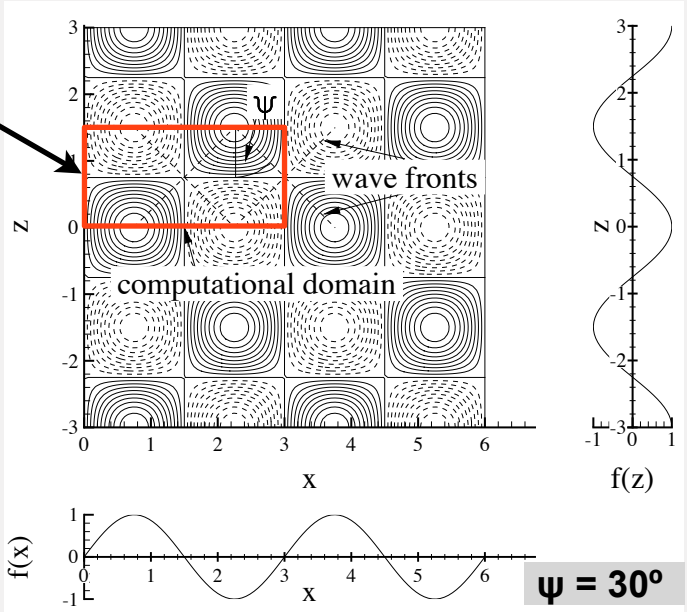
- forcing function

$$f(x,y,z,t) = \cos(\omega_r t)\, e^{-\left(\frac{y-y_{vf}}{\sigma_y}\right)^2} \sum_{i=1}^{n_{forcing}} A_{forcing,i} \sin(m_{x,i}\alpha_r x) \cos\left(m_{z,i}\frac{\beta_r}{2} z\right)$$

- ω_r: frequency
- $\alpha_r = 2\,\pi/\lambda_x$: streamwise wavenumber
- $\beta_r = 2\,\pi/\lambda_z$: spanwise wavenumber
- fundamental wavenumber defined by domain size (L_x, L_z)
- $\alpha_{fund} = 2\,\pi/L_x$; $\beta_{fund} = 2\,\pi/L_z$
- wave angle is controlled by extent of computational domain

$$\psi = \arctan\left(\frac{\beta_r}{\alpha_r}\right)$$





Base Flow and Disturbance Generation

- forcing function

$$f(x,y,z,t) = \cos(\omega_r t)\, e^{-\left(\frac{y-y_{vf}}{\sigma_y}\right)^2} \sum_{i=1}^{n_{forcing}} A_{forcing,i} \sin(m_{x,i}\alpha_r x) \cos\left(m_{z,i}\frac{\beta_r}{2} z\right)$$

- ω_r: frequency
- $\alpha_r = 2\,\pi/\lambda_x$: streamwise wavenumber
- $\beta_r = 2\,\pi/\lambda_z$: spanwise wavenumber
- fundamental wavenumber defined by domain size (L_x, L_z)
- $\alpha_{fund} = 2\,\pi/L_x$; $\beta_{fund} = 2\,\pi/L_z$
- wave angle is controlled by extent of computational domain

Terminology

mode (n,m)

$\alpha_{n,m} = n \cdot \alpha_{fund}$

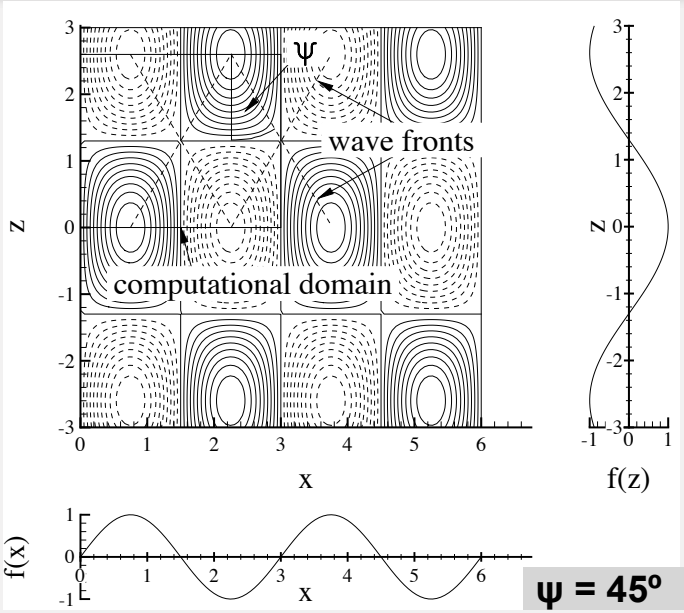
$\lambda_x = L_x/n$

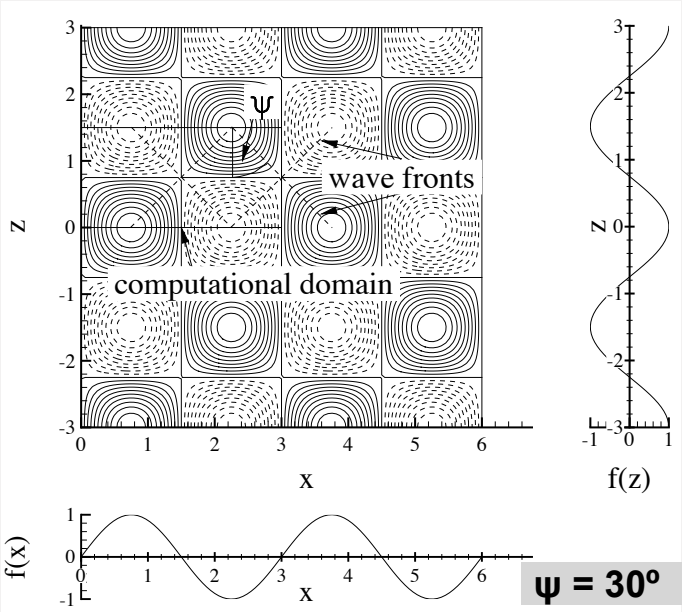
n = 0 ⇒ 90° wave

$\beta_{n,m} = m \cdot \beta_{fund}$

$\lambda_z = L_z/m$

m = 0 ⇒ 0° wave





Intermediate Summary



- Higher order finite differences for inviscid and viscous terms
- Perfect gas
- Higher order Immersed Boundary Method to physically resolve porous walls
- Temporal Simulations
- M = 6 Base Flow
- Freestream temperature of T = 216.65 K (cold flow)
- Volume forcing to introduce disturbances
- (n,m) mode terminology important for later discussions

Outline



Introduction/Motivation

Governing Equations and Numerical Methods

Base Flow and Disturbance Generation

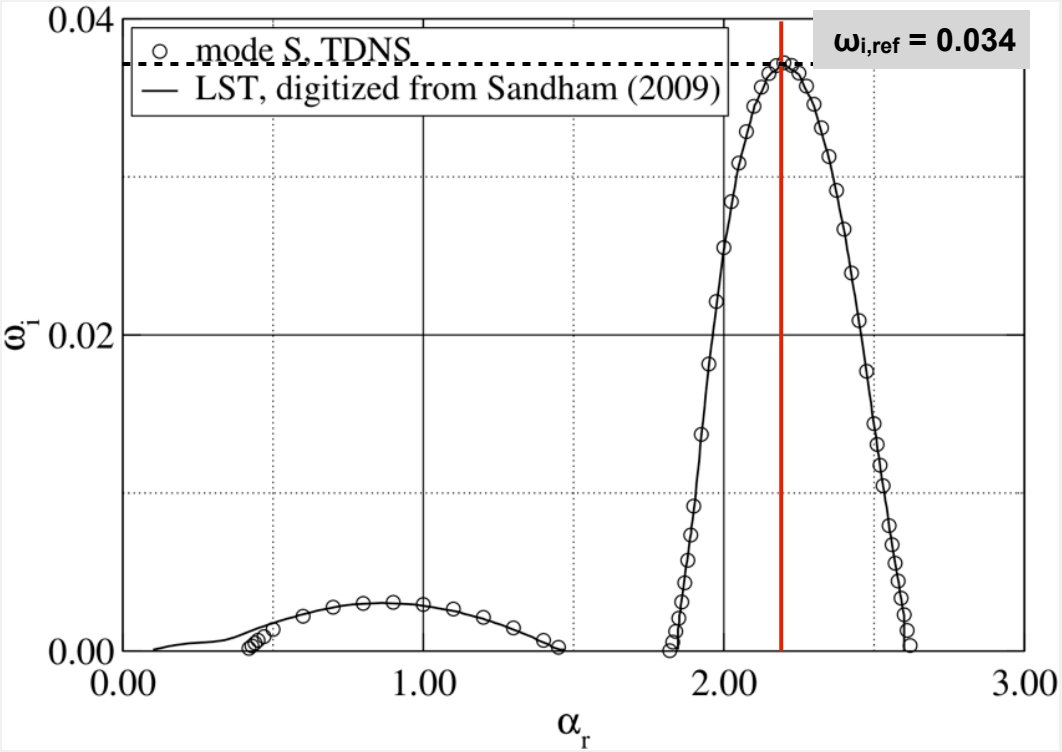
Linear Regime

Nonlinear Regime

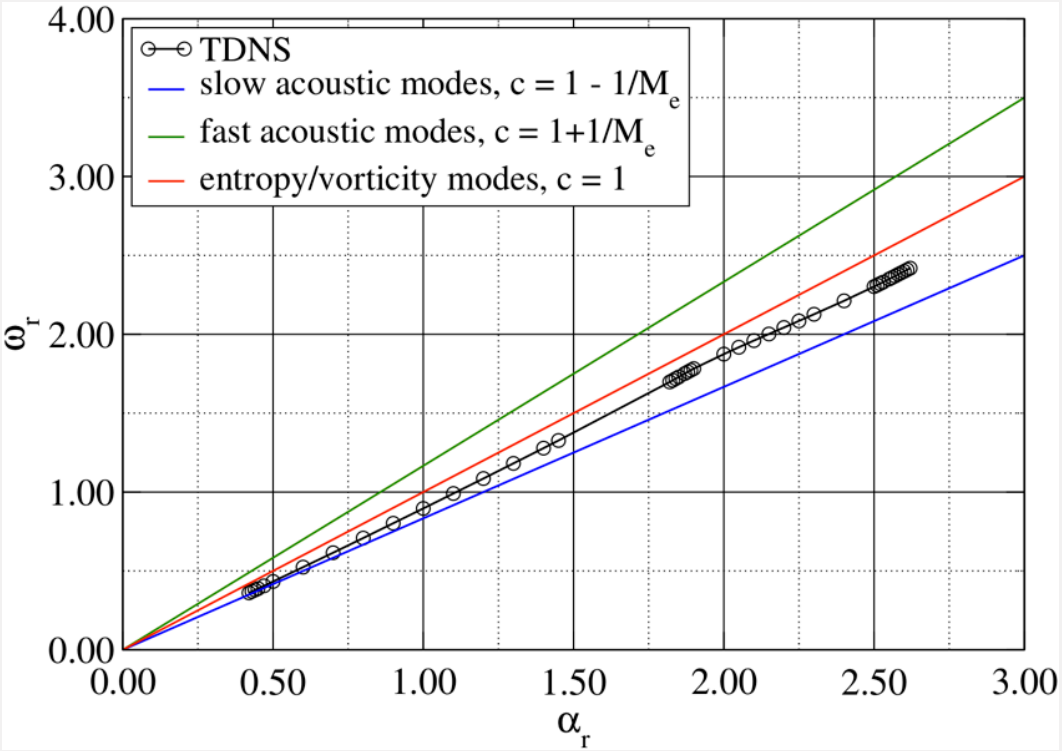
Summary

Smooth wall

- Identify most amplified disturbance, 2D, mode (1,0)
- Two unstable regions (first mode/second mode)
- Most amplified case: $\lambda_x = 3$ corresponding to $\alpha \approx 2.09$



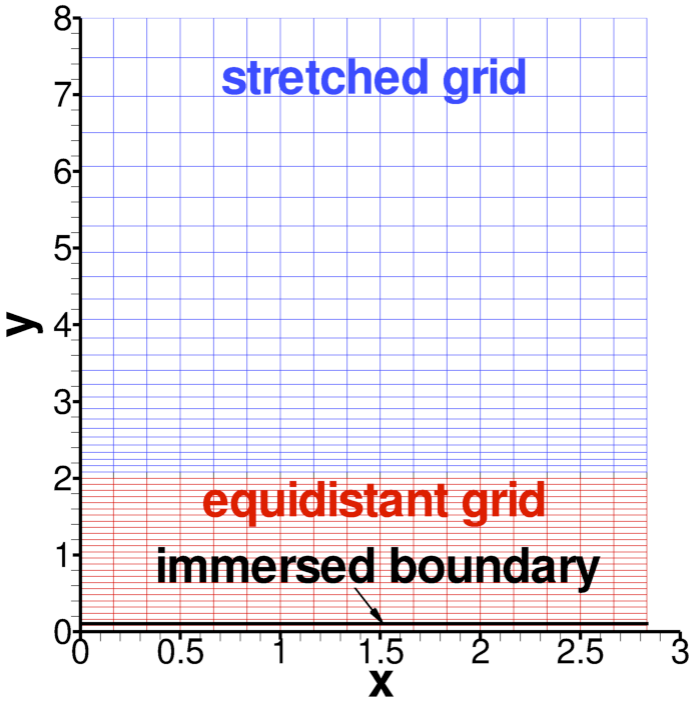
Temporal growth rate vs streamwise wavenumber (mode (1,0))



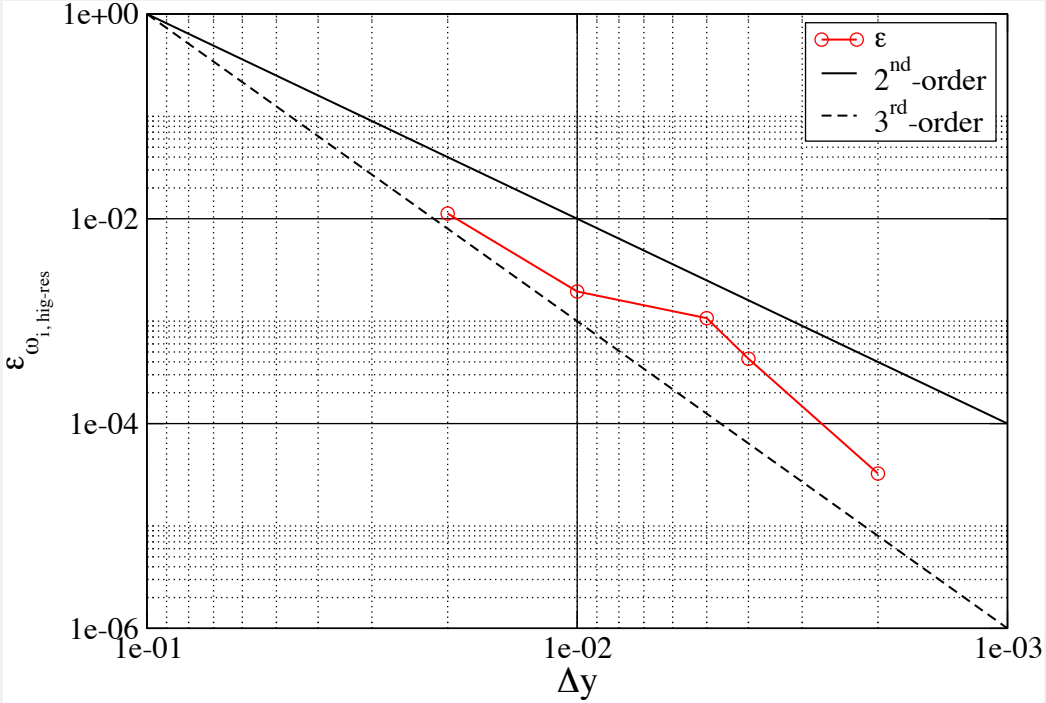
Frequency vs streamwise wavenumber (mode (1,0))

Immersed Boundary: Validation

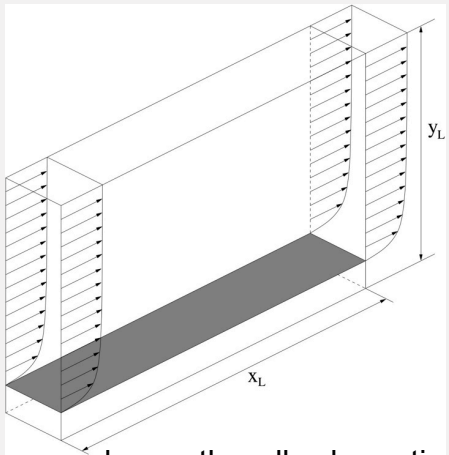
- Immersed smooth wall at y = 0.1
- Equidistant grid up to y = 2.0 to avoid grid stretching effects
- immersed boundary scheme converges with order > 2



Grid schematic



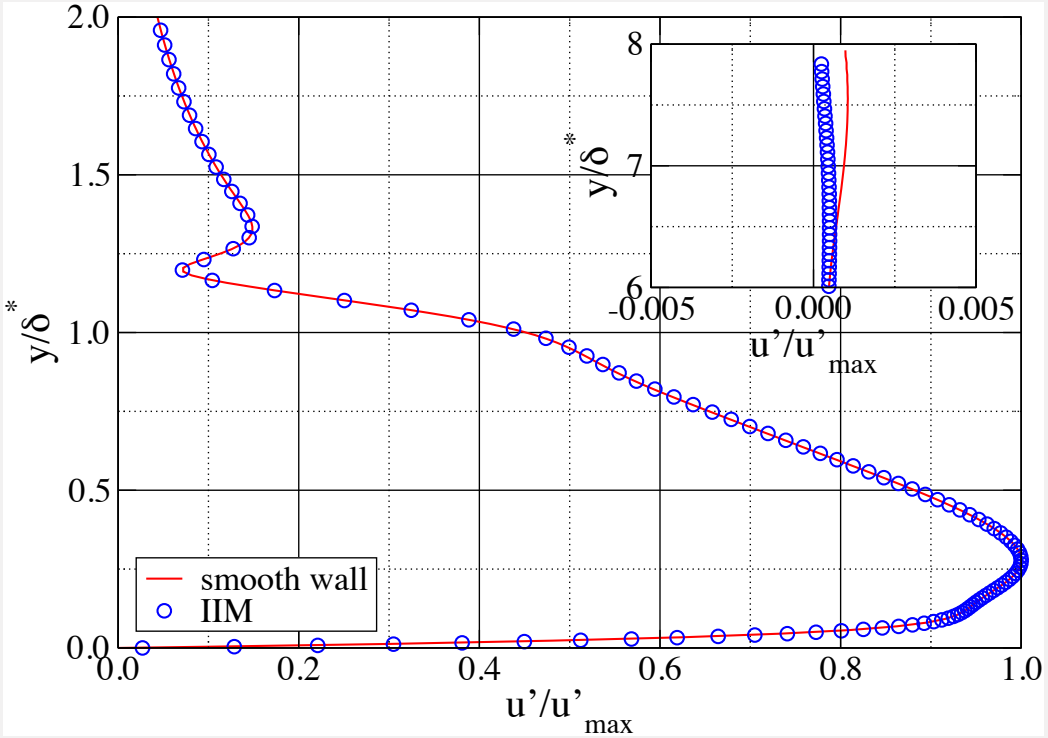
Error convergence of temporal growth rate.



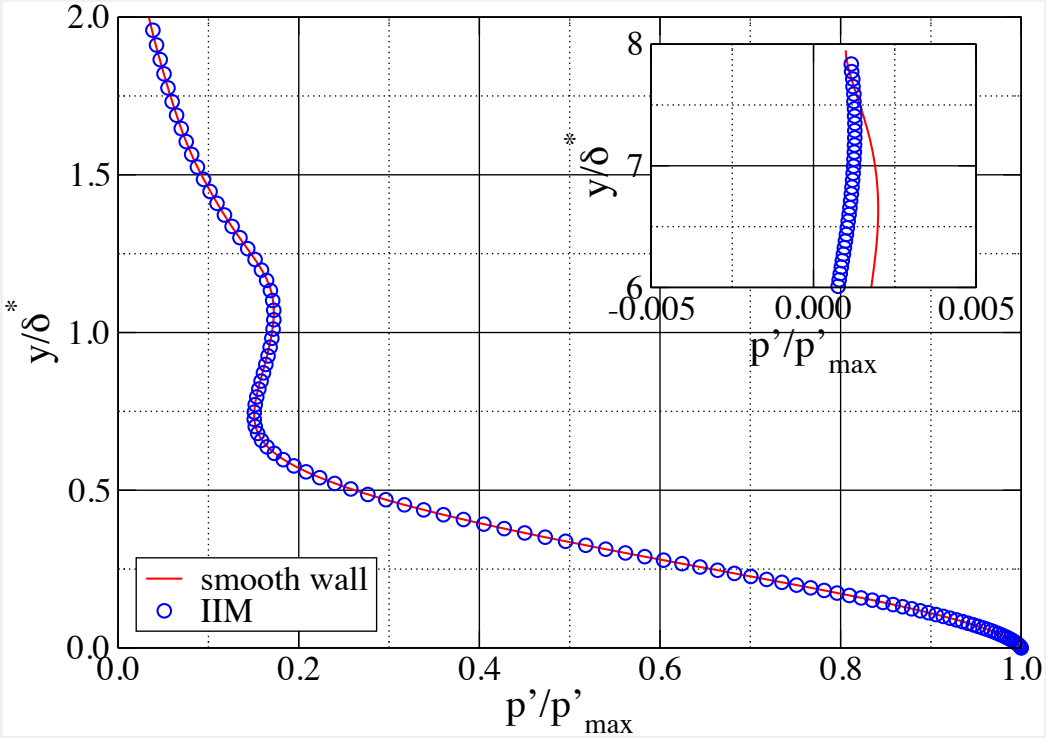
Immersed smooth wall schematic.

Immersed Boundary: Validation

- Excellent match between amplitude distributions with body fitted grid and immersed boundary method
- Decay of amplitude distributions to zero at free stream boundary



Comparison of normalized streamwise velocity disturbance amplitude distributions for immersed smooth wall and a body fitted grid

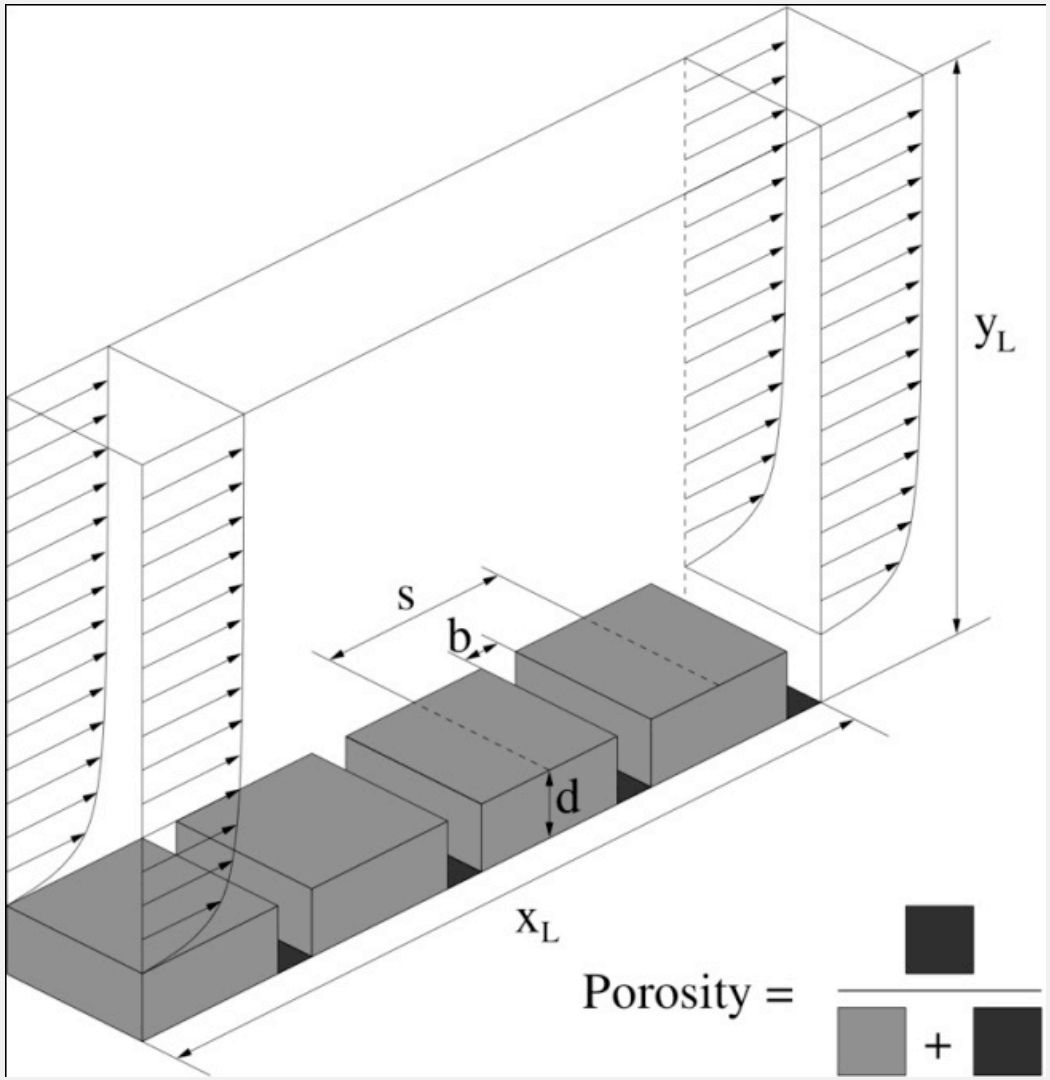


Comparison of normalized pressure disturbance amplitude distributions for immersed smooth wall and a body fitted grid

Porous Wall Parameters

Porous wall parameters:

- b = pore width
- d = pore depth
- n_p = number of pores per disturbance wavelength
- φ = porosity



Schematic of porous wall

Grid Convergence Study



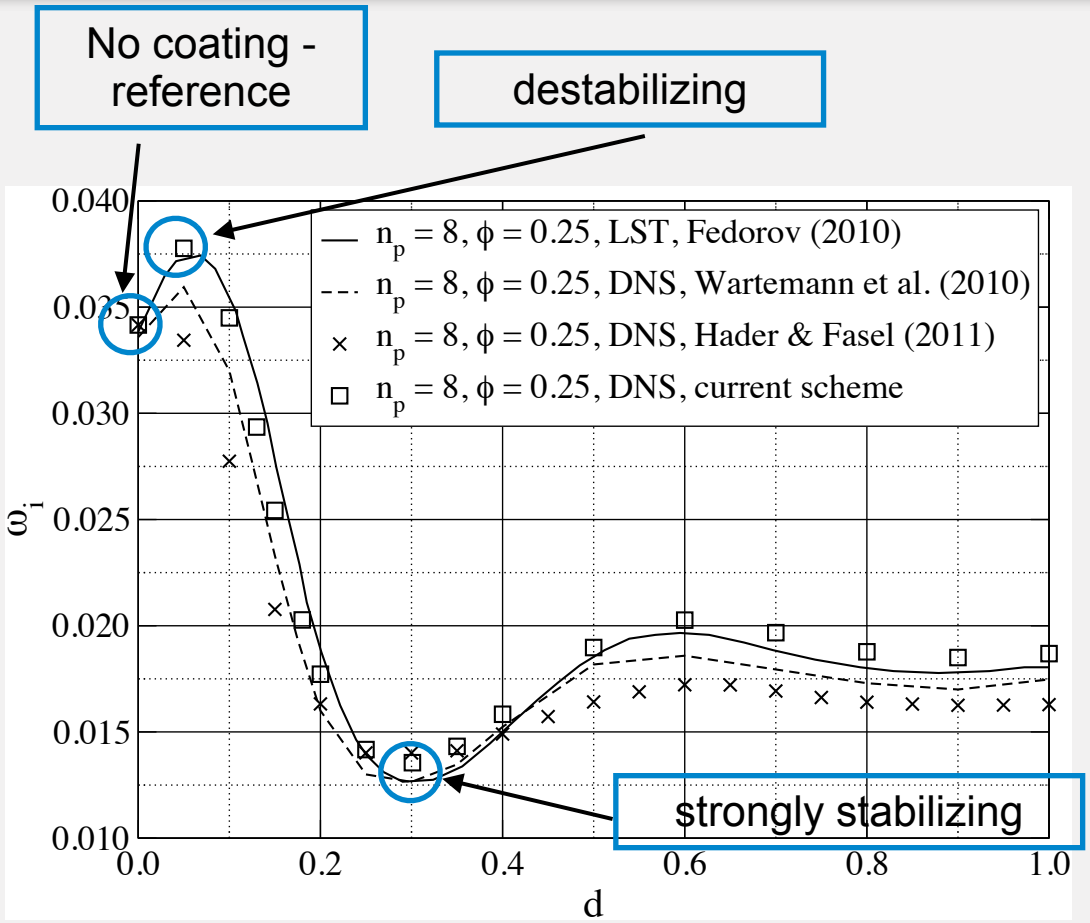
- Fix number of pores per wavelength and cavity depth
- variation of number of points per pore (n_{pore})
- Average temporal growth rate
- approximately 100 points in wall normal direction within cavity

n_p	d	ϕ	x_L	n_x	n_{pore}	$\omega_{\text{i,avg1}}$	ϵ_{avg1}	order	$\omega_{\text{i,avg2}}$	ϵ_{avg2}	order
8	0.3	0.25	3	384	12	0.013724	0.0176	2.74	0.013255	0.0190	2.75
8	0.3	0.25	3	480	15	0.013644	0.0117	3.46	0.013172	0.0127	3.47
8	0.3	0.25	3	640	20	0.013545	0.0043	-	0.013068	0.0047	-
8	0.3	0.25	3	800	25	0.013487	-	-	0.013008	-	-

Results of grid study in steamwise direction

Porous Wall Simulations (2D)

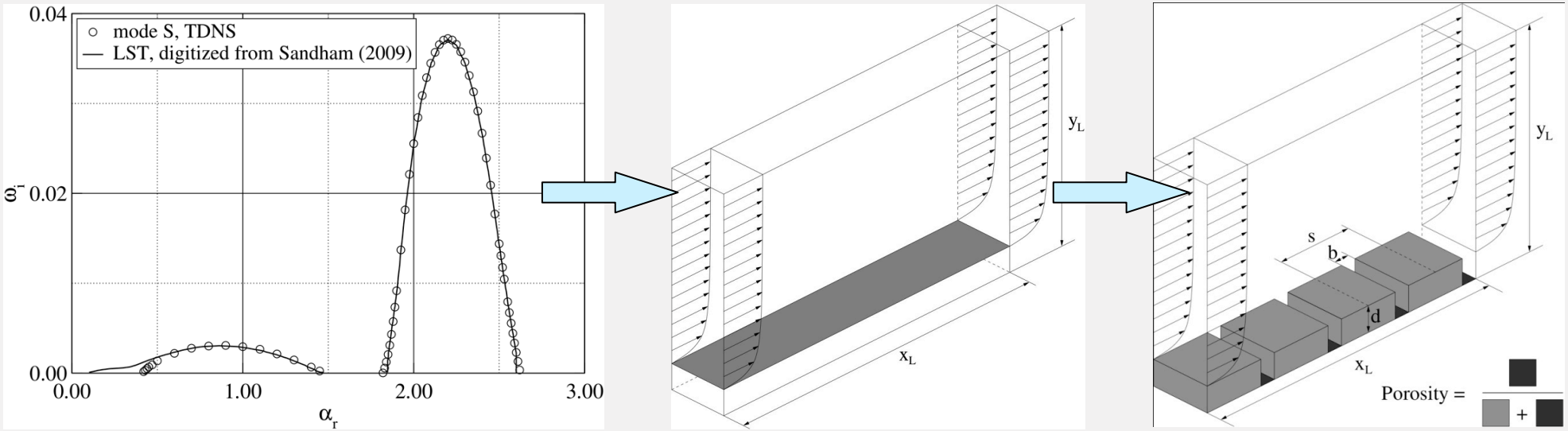
- Good match of temporal growth rates obtained with immersed boundary approach and LST results by Fedorov
- Porous walls are destabilizing for narrow cavities
- Maximum stabilization for d = 0.3
- For sufficiently deep pores the effect of a further increase in cavity depth becomes small



Temporal growth rate versus cavity depth for $n_p = 8$ and $\varphi = 0.25$.

Intermediate Summary

- Find most amplified disturbance
- Convergence study to find wall normal grid spacing needed at the immersed boundary
- Convergence study to find number of points needed across a cavity
- Good match between results obtained with Immersed Boundary Method and previous studies



Outline



Introduction/Motivation

Governing Equations and Numerical Methods

Base Flow and Disturbance Generation

Linear Regime

Nonlinear Regime

Summary

Nonlinear Regime

- Initiating breakdown through so called controlled breakdown scenarios
- Focus here on fundamental and subharmonic resonance scenario
- Forcing of a primary (2D) and secondary (3D) disturbance wave at small amplitudes

Fundamental Resonance

- Primary wave: mode (1,0)
- Secondary wave: mode (1,1)

$$\alpha_{r(1,1)} = \alpha_{r(1,0)}$$

$$\omega_{r(1,1)} = \omega_{r(1,0)}$$

Subharmonic Resonance

- Primary wave: mode (2,0)
- Secondary wave: mode (1,1)

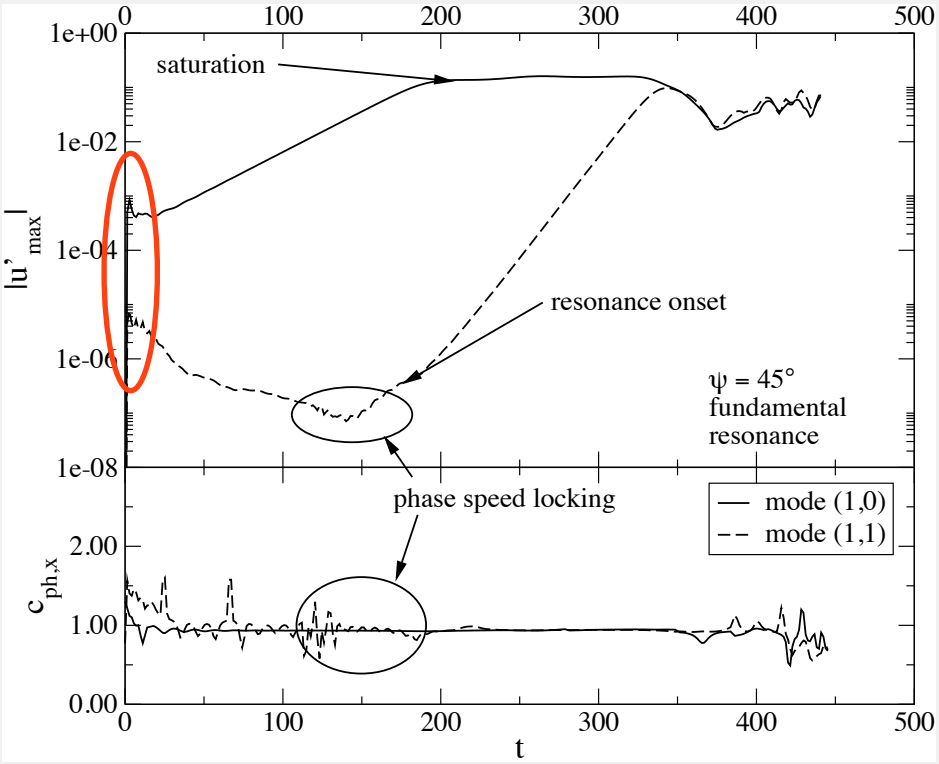
$$\alpha_{r(1,1)} = \alpha_{r(2,0)}/2$$

$$\omega_{r(1,1)} = \omega_{r(2,0)}/2$$

Controlled Breakdown Scenarios

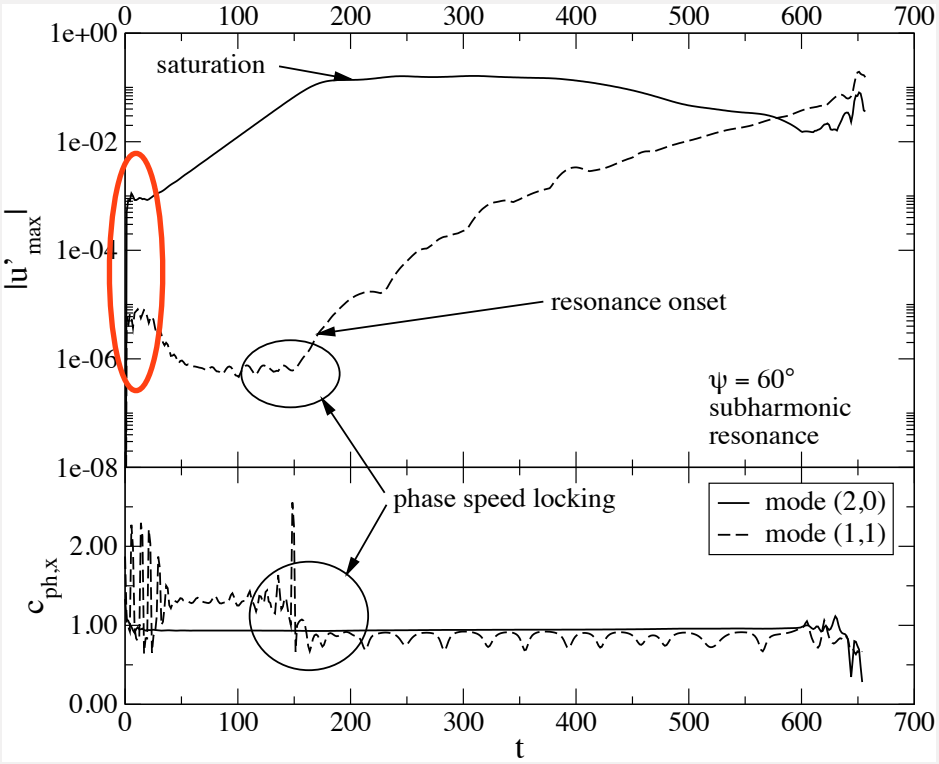
- Forcing amplitudes: $A_{(1,0)} = 10^{-3}$, $A_{(1,1)} = 10^{-5}$
- phase speed locking → resonance
- 'better' phase speed match seems to lead to stronger resonance

fundamental resonance



Maximum disturbance amplitude and disturbance phase speed vs. time

subharmonic resonance

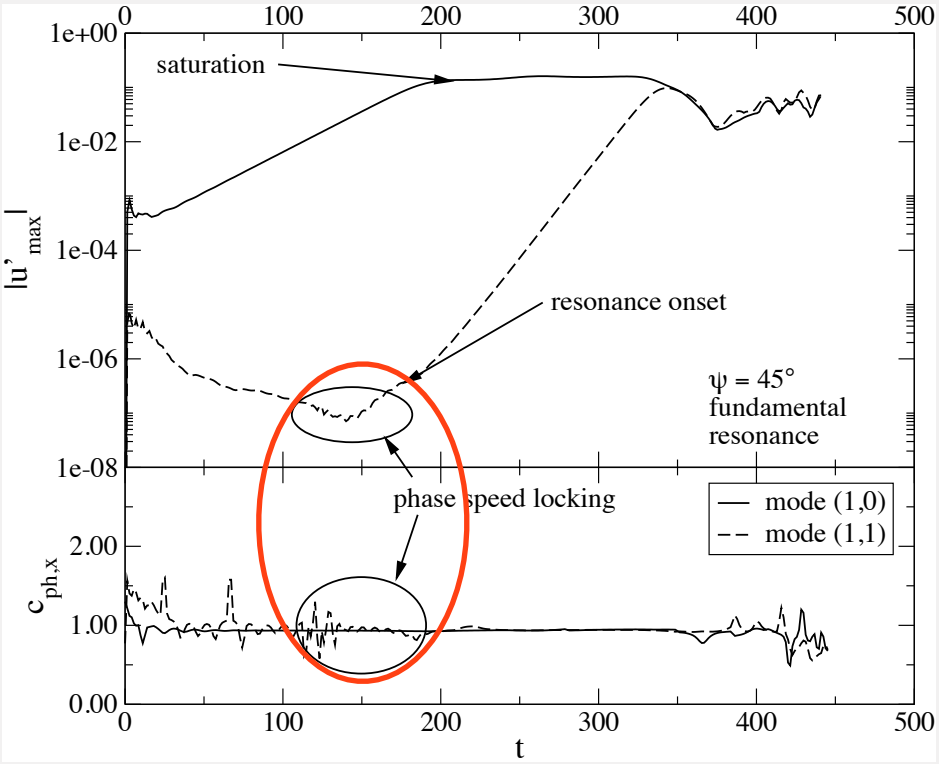


Maximum disturbance amplitude and disturbance phase speed vs. time

Controlled Breakdown Scenarios

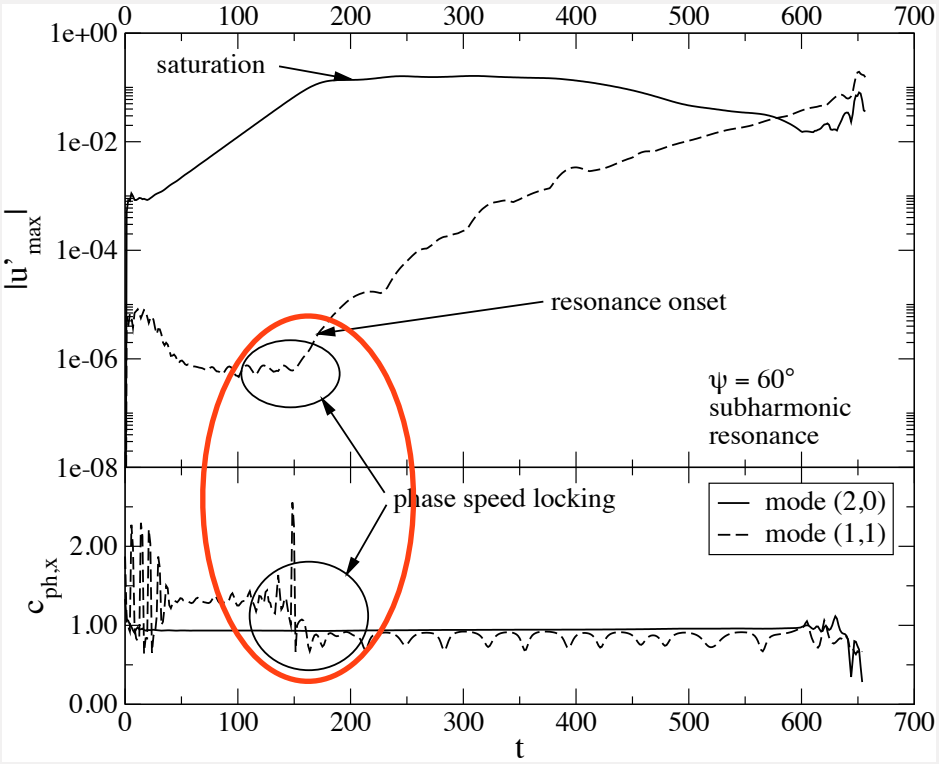
- Forcing amplitudes: $A_{(1,0)} = 10^{-3}$, $A_{(1,1)} = 10^{-5}$
- phase speed locking → resonance
- 'better' phase speed match seems to lead to stronger resonance

fundamental resonance



Maximum disturbance amplitude and disturbance phase speed vs. time

subharmonic resonance

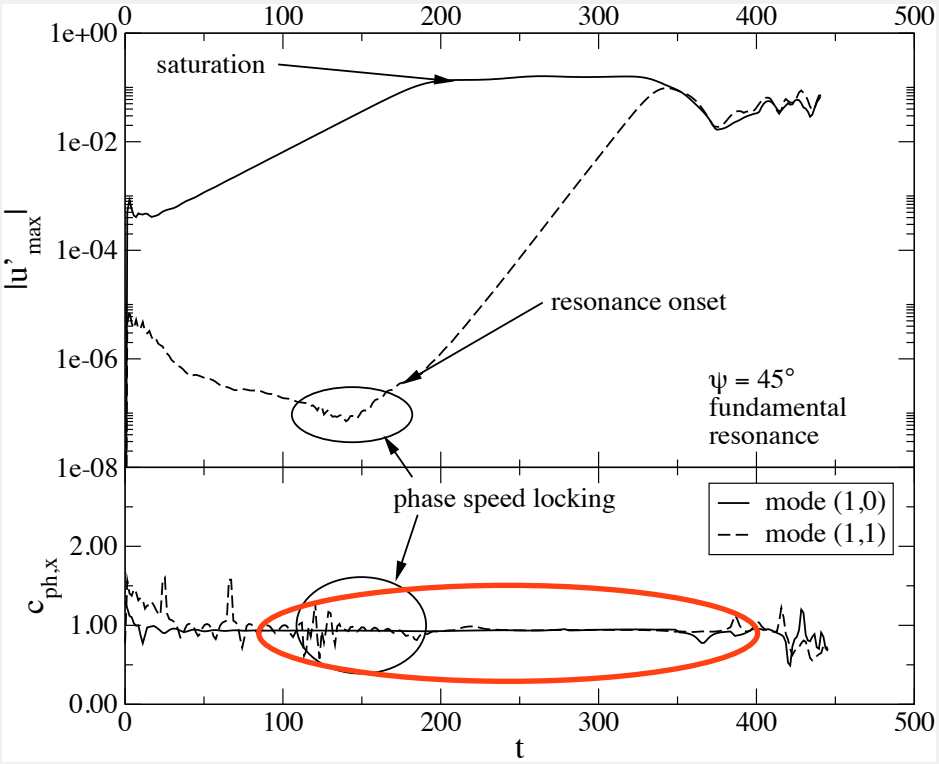


Maximum disturbance amplitude and disturbance phase speed vs. time

Controlled Breakdown Scenarios

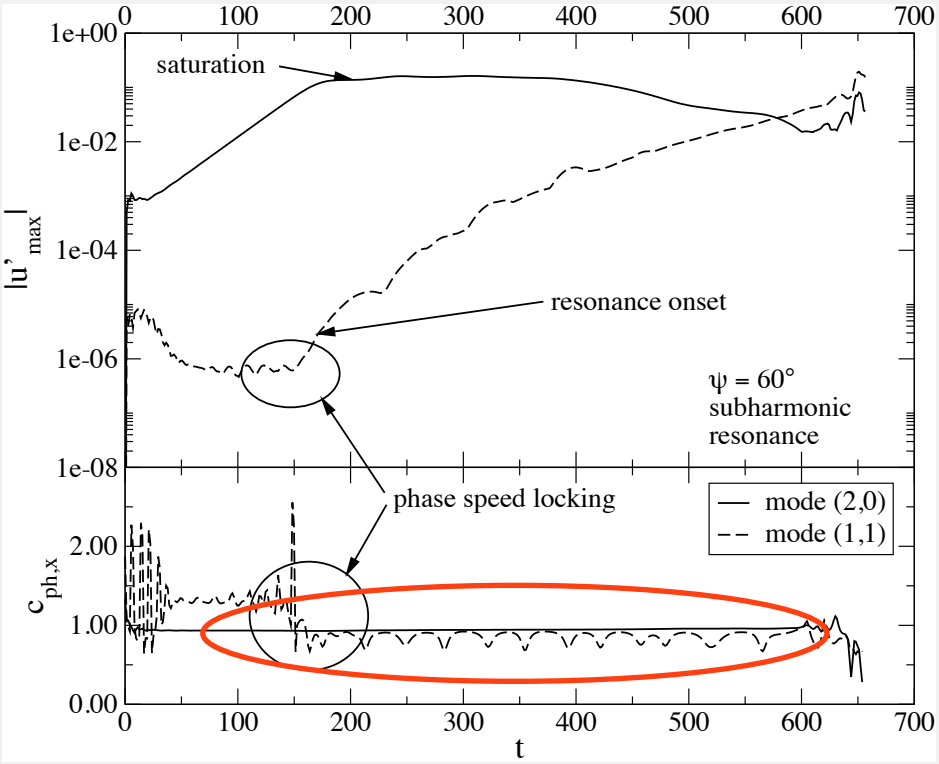
- Forcing amplitudes: $A_{(1,0)} = 10^{-3}$, $A_{(1,1)} = 10^{-5}$
- phase speed locking → resonance
- 'better' phase speed match seems to lead to stronger resonance

fundamental resonance



Maximum disturbance amplitude and disturbance phase speed vs. time

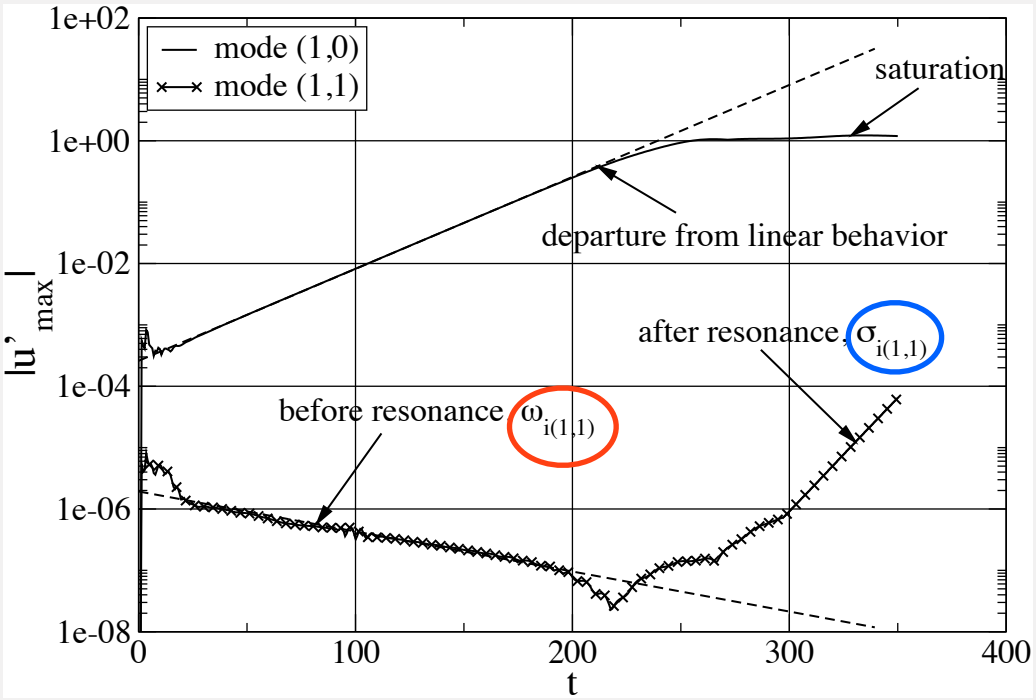
subharmonic resonance



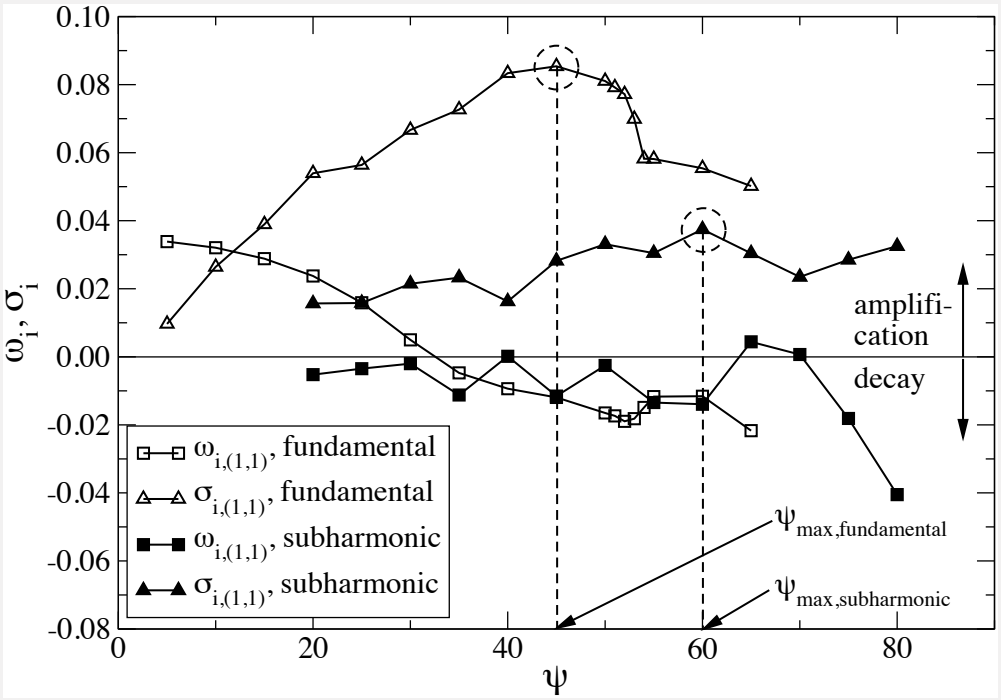
Maximum disturbance amplitude and disturbance phase speed vs. time

Parameter Study

- find wave angle of mode (1,1) for which growth rate after the resonance onset becomes maximal
- growth rate of secondary wave before resonance onset: $\omega_{i(1,1)}$
- growth rate of secondary wave after resonance onset: $\sigma_{i(1,1)}$
- fundamental resonance: strongest resonance for ψ = 45°
- subharmonic resonance: strongest resonance for ψ = 60°



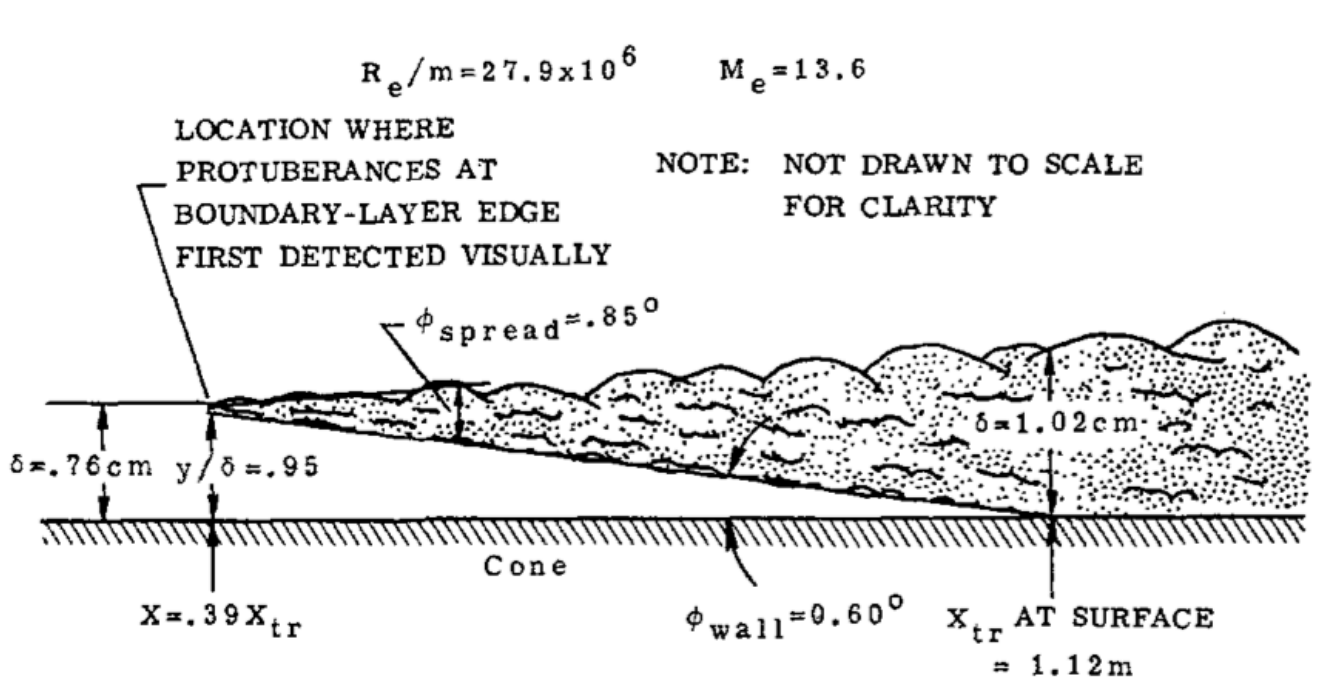
Maximum disturbance amplitude of primary and secondary wave over time



Growth rate before and after resonance onset of secondary wave

Simulation Setup (wall normal grid)

- Before running breakdown simulations identify regions where wall normal grid needs to be highly resolved
- Near wall resolution critical
- Transition occurs first at critical layer: ‘precursor transition’ (*Pruett & Zang 1992*)
- Resolution at critical layer important



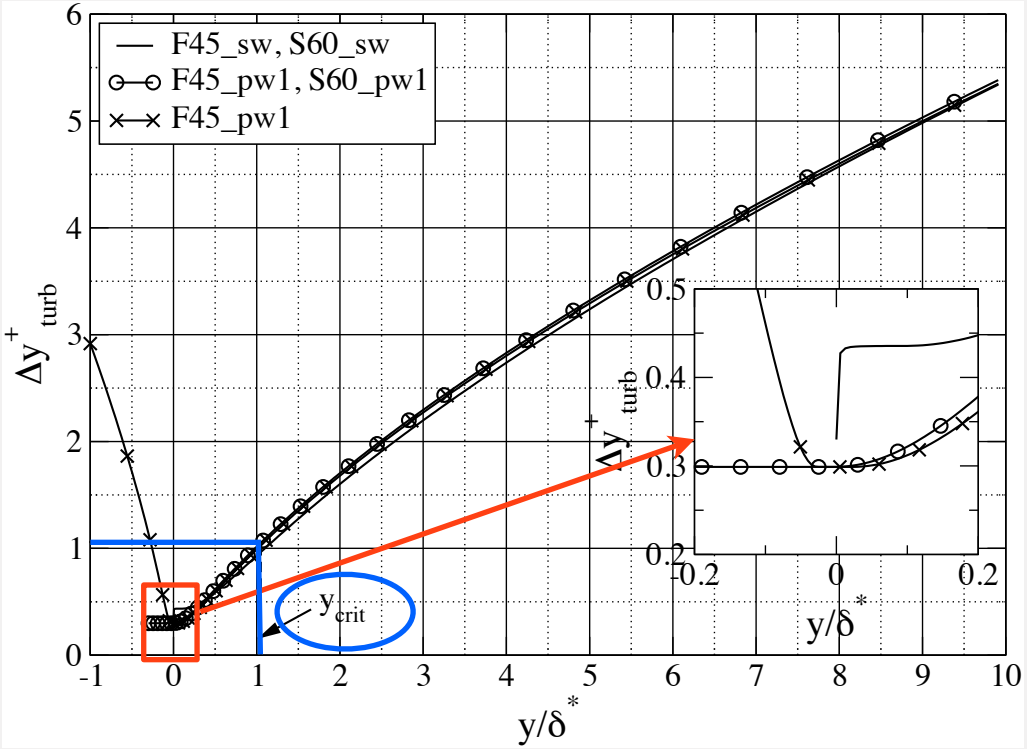
Schematic of turbulent spot development in high speed flow (*Fischer & Weinstein (1972)*)

Simulation Setup (wall normal grid)

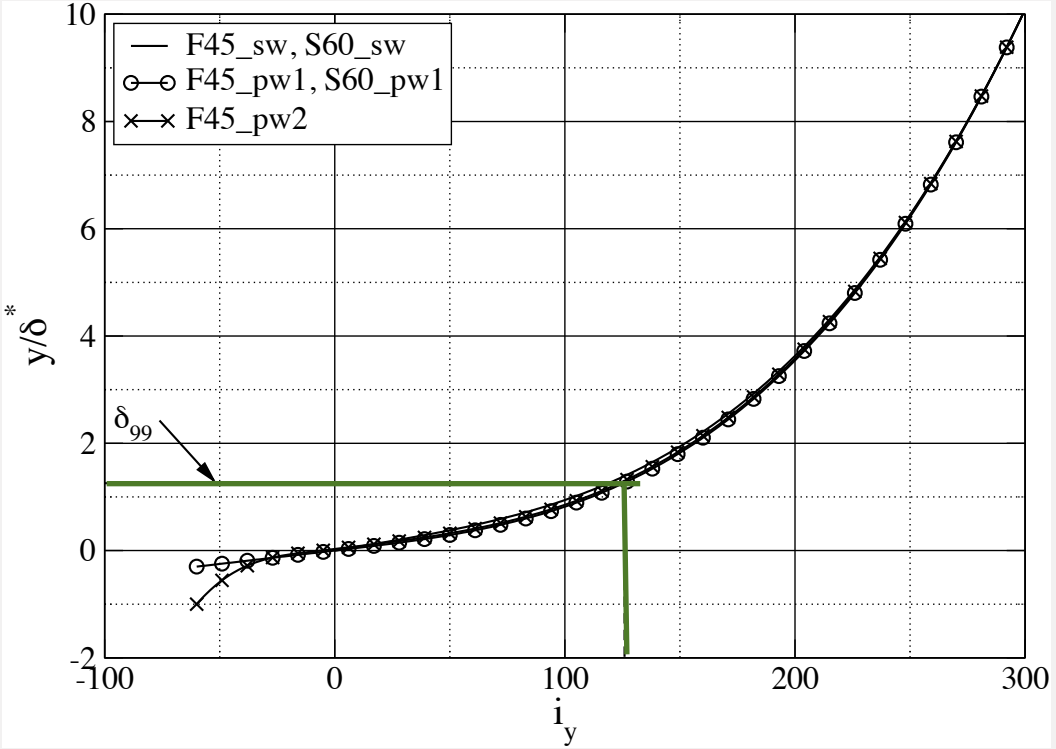
- Rescale grid spacing with friction velocity based on turbulent estimate of skin friction

$$\Delta y^+_{\text{turb}} = (y_j - y_{j-1}) \frac{Re}{\nu_w} \sqrt{\frac{c_{f,\text{turb}} \rho_w}{2}}$$

- $\Delta y^+ \approx 0.3$ at the **wall**
- $\Delta y^+ \approx 1$ at **critical layer**
- Approximately 130 points within **Boundary Layer**



Rescaled grid spacing vs. wall normal coordinate



Wall normal coordinate vs. grid index j

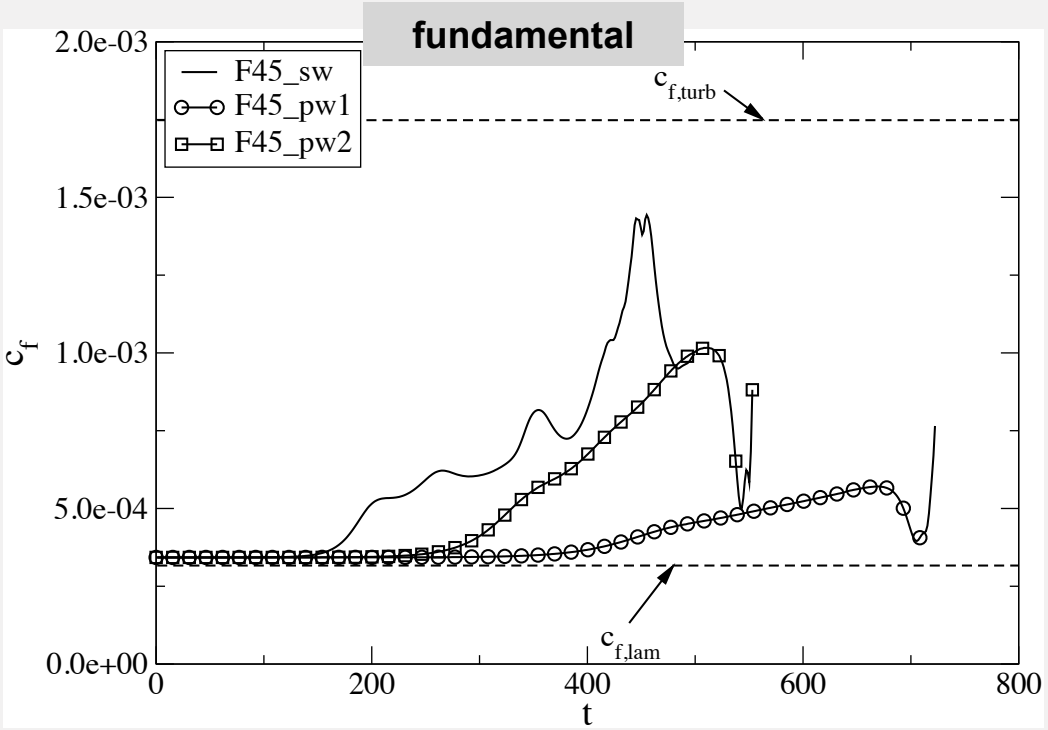
Simulations

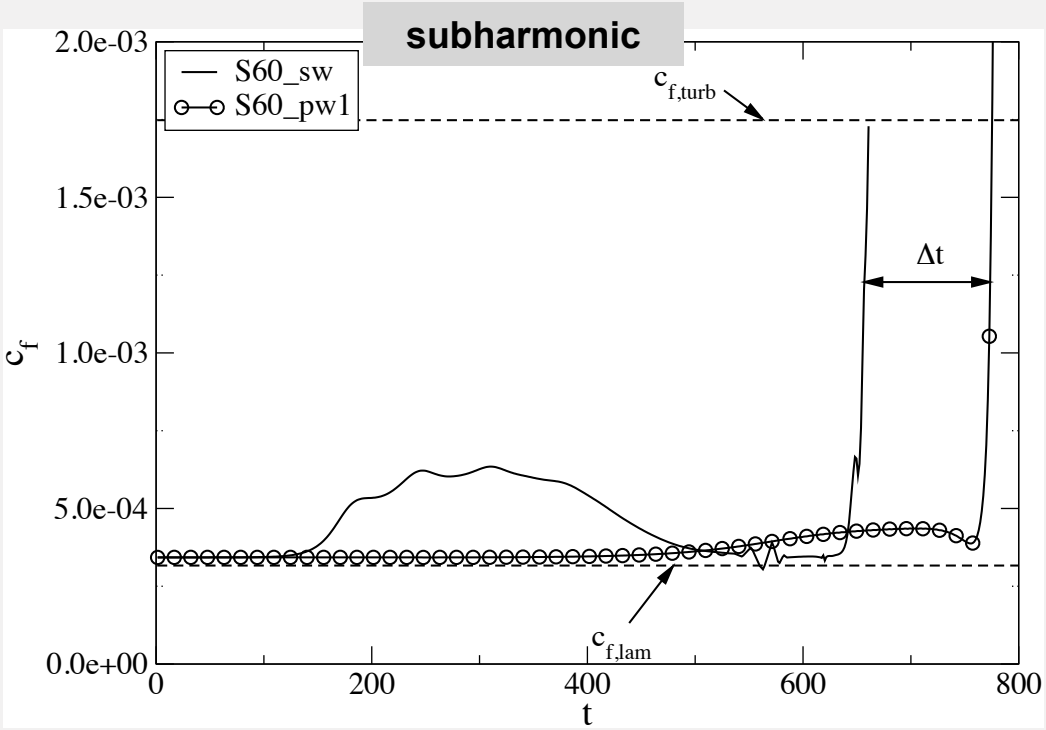
Case	Breakdown	Geometry	λ_x/δ^*	λ_z/δ^*	n_y	$\psi_{1,1}$	forcing amplitudes
F45_sw	Fundamental	smooth wall	3.0000	3.0000	300	45°	$A_{1,0} = 10^{-3}$, $A_{1,1} = 10^{-5}$
F45_pw1	Fundamental	$n_p = 8, d = 0.30, \phi = 0.25$	3.0000	3.0000	360	45°	$A_{1,0} = 10^{-3}$, $A_{1,1} = 10^{-5}$
F45_pw2	Fundamental	$n_p = 8, d = 1.00, \phi = 0.25$	3.0000	3.0000	360	45°	$A_{1,0} = 10^{-3}$, $A_{1,1} = 10^{-5}$
S60_sw	Subharmonic	smooth wall	6.0000	3.4641	300	60°	$A_{2,0} = 10^{-3}$, $A_{1,1} = 10^{-5}$
S60_pw1	Subharmonic	$n_p = 8, d = 0.30, \phi = 0.25$	6.0000	3.4641	360	60°	$A_{2,0} = 10^{-3}$, $A_{1,1} = 10^{-5}$

- F: fundamental resonance
- S: subharmonic resonance
- 45: ψ = 45º
- 60: ψ = 60º
- sw: smooth wall
- pw1: porous wall setup 1; n_p = 8, **d = 0.30**, φ = 0.25
- pw2: porous wall setup 2; n_p = 8, **d = 1.00**, φ = 0.25

Skin friction evolution

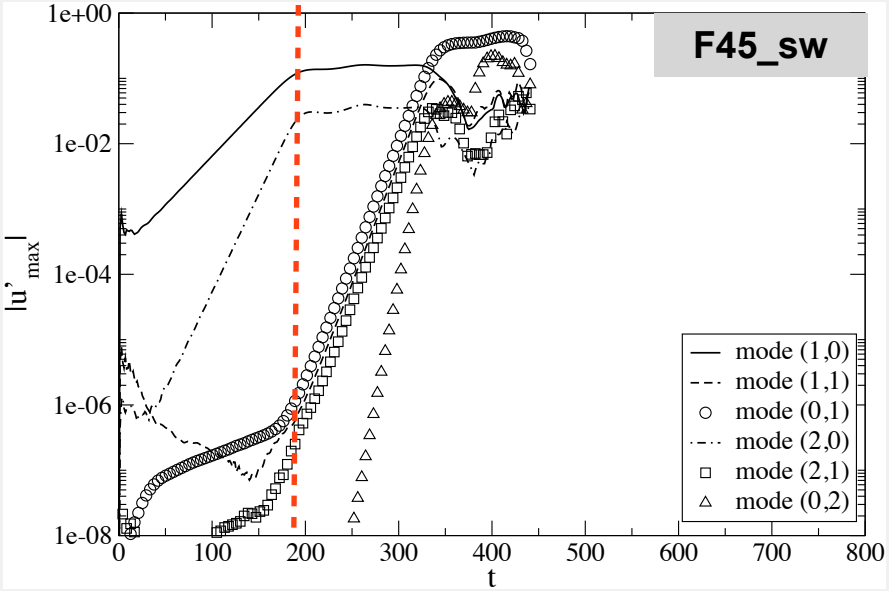
- transition onset (time where c_f departs from its laminar value) significantly delayed due to porous walls for both resonance scenarios
- skin friction evolution altered by presence of porous walls
- skin friction for S60_sw drops back to laminar value before rapidly approaching turbulent estimate
- S60_pw1 significantly delays transition

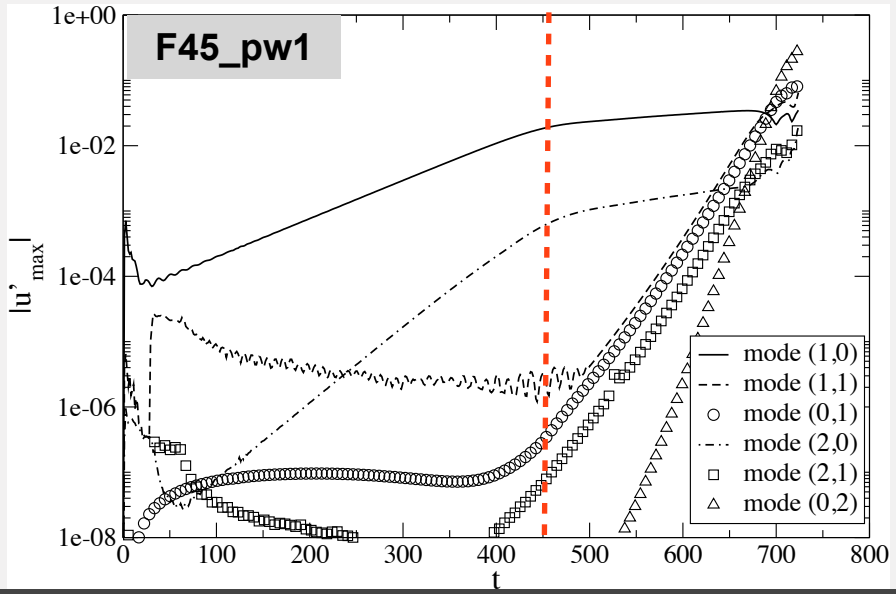


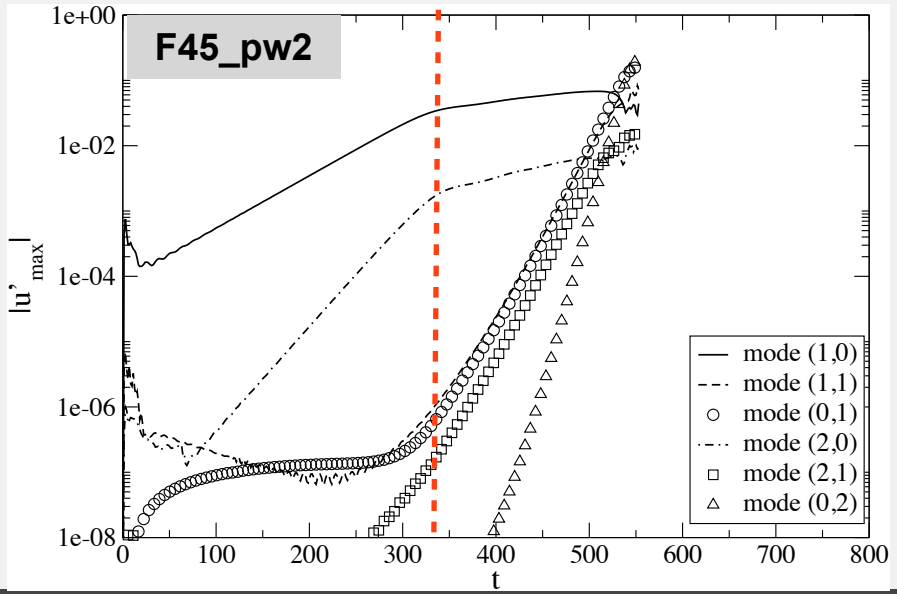


Amplitude evolution (fundamental)

- amplitude evolution altered, ‘saturation’ occurs at much later time
- mode (1,0) keeps growing slightly for porous wall cases
- mode (0,2) becomes dominant along with mode (0,1)

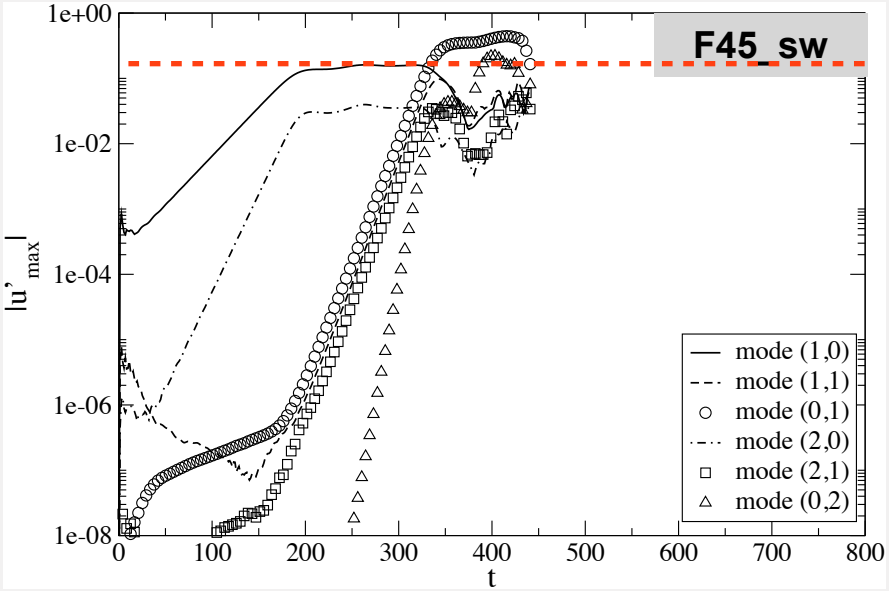


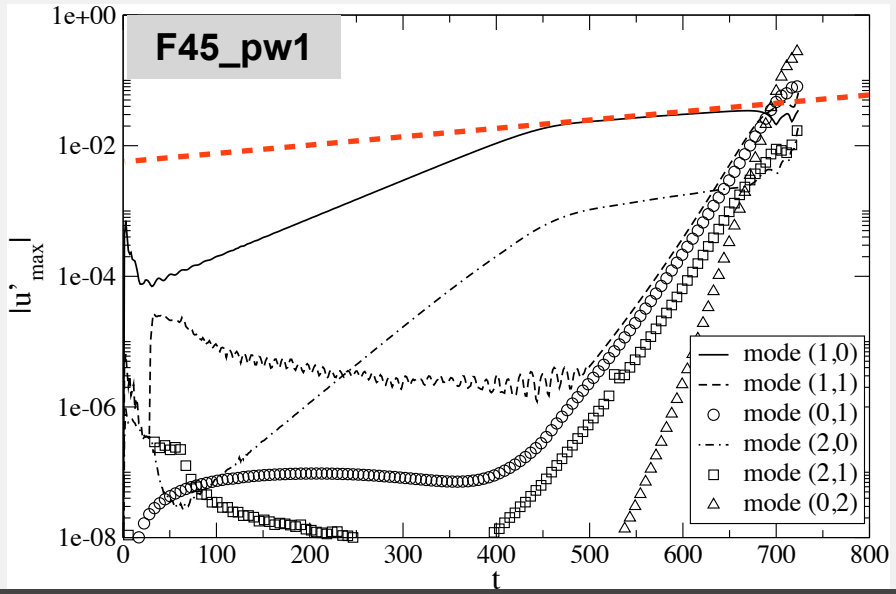


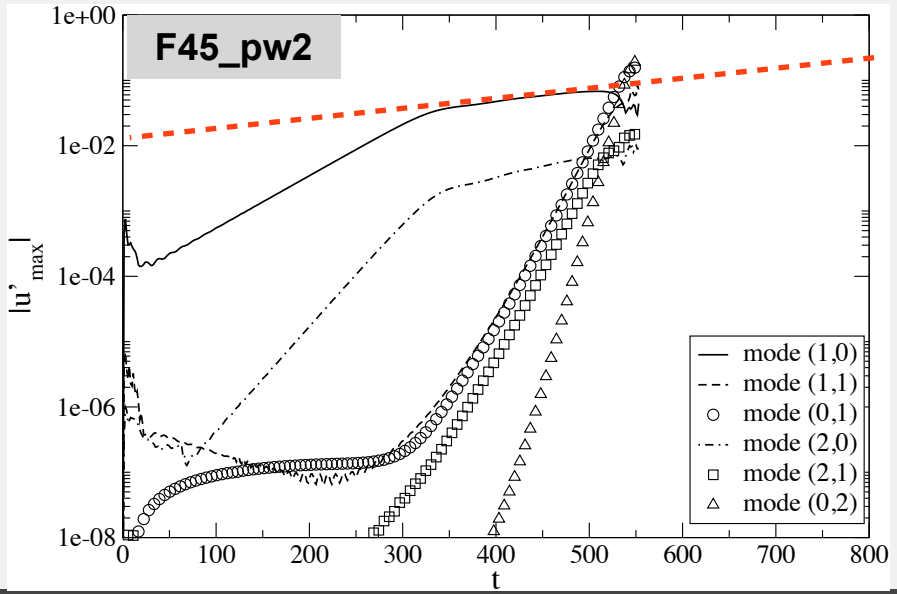


Amplitude evolution (fundamental)

- amplitude evolution altered, ‘saturation’ occurs at much later time
- mode (1,0) keeps growing slightly for porous wall cases
- mode (0,2) becomes dominant along with mode (0,1)

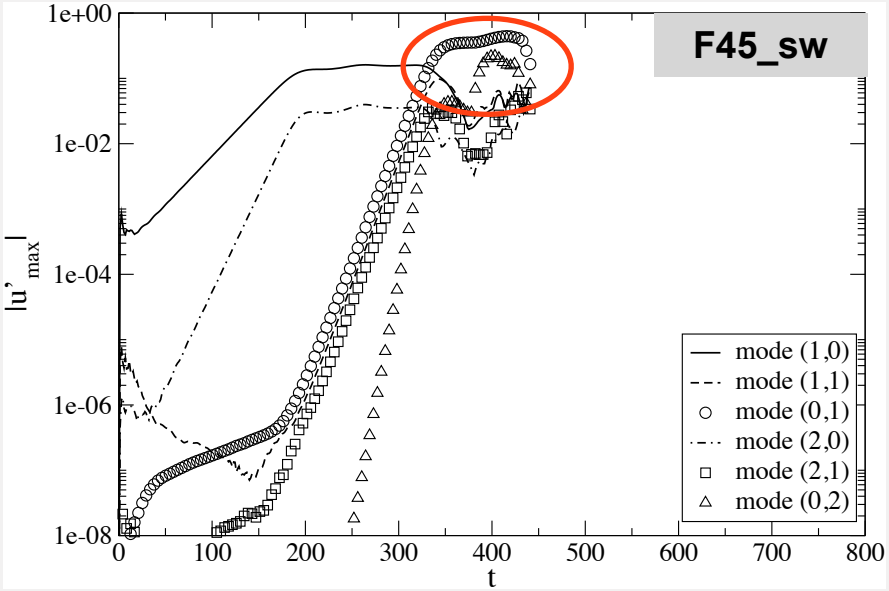


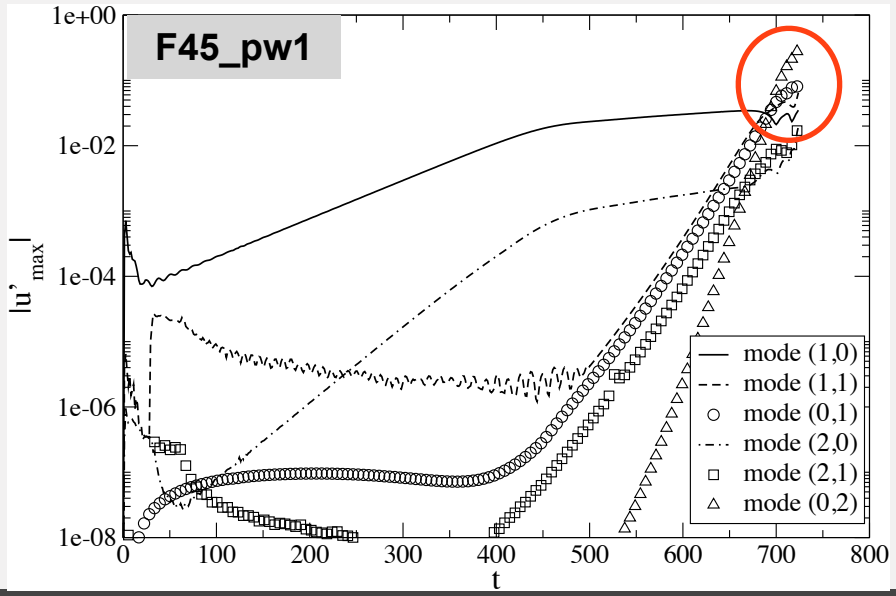


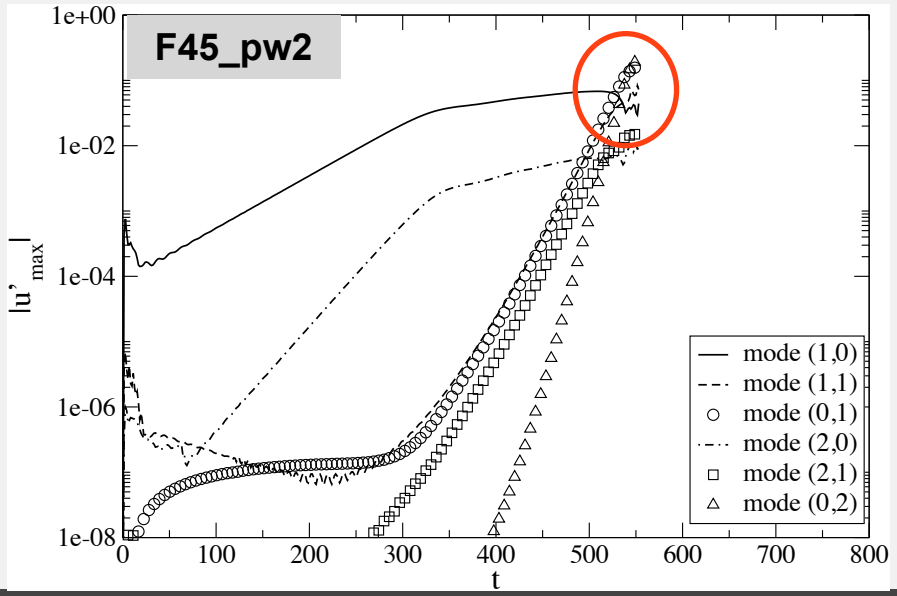


Amplitude evolution (fundamental)

- amplitude evolution altered, ‘saturation’ occurs at much later time
- mode (1,0) keeps growing slightly for porous wall cases
- mode (0,2) becomes dominant along with mode (0,1)



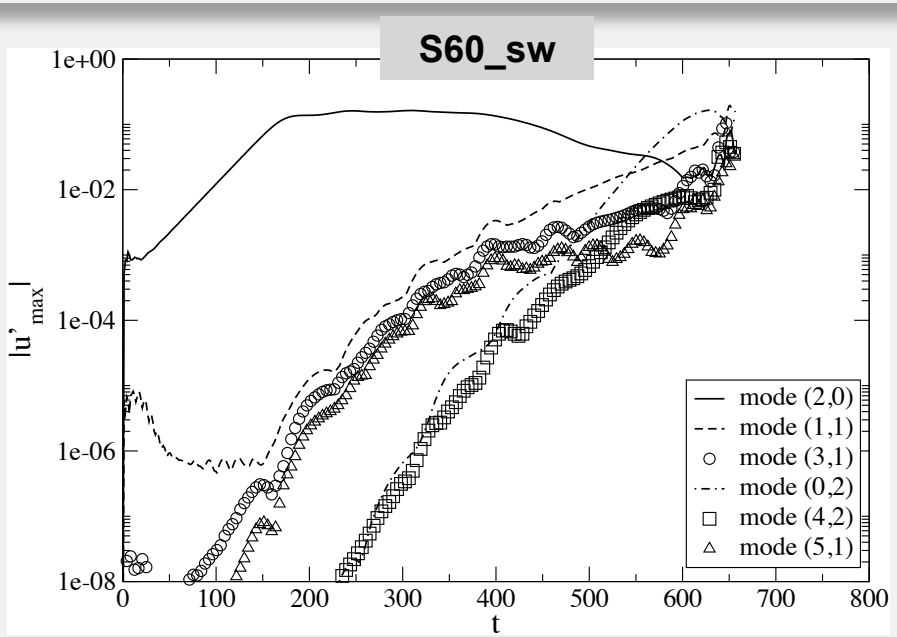


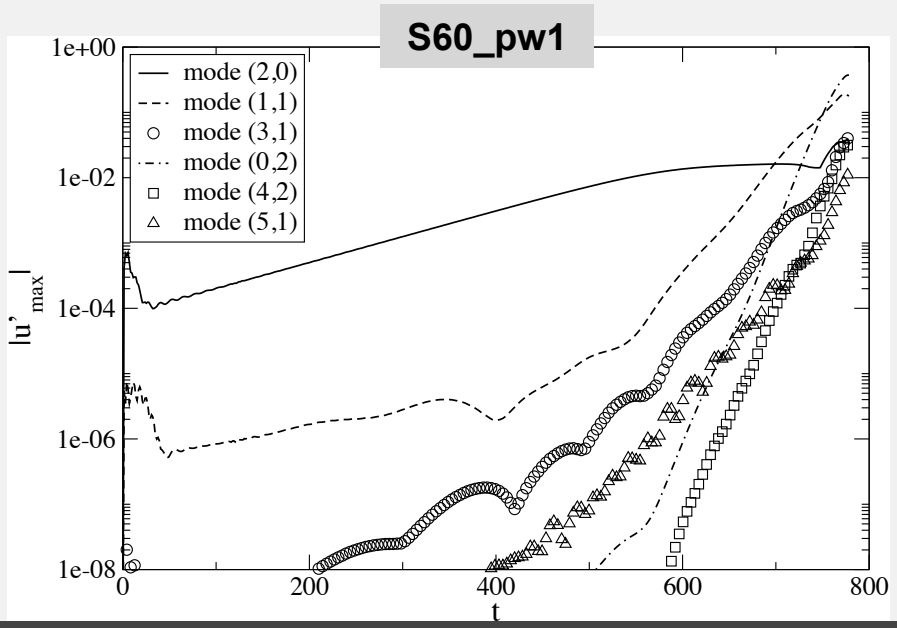


Amplitude evolution (subharmonic)

- similar to fundamental resonance case
- primary wave keeps growing for porous wall case
- presence of porous wall significantly alters mode evolution

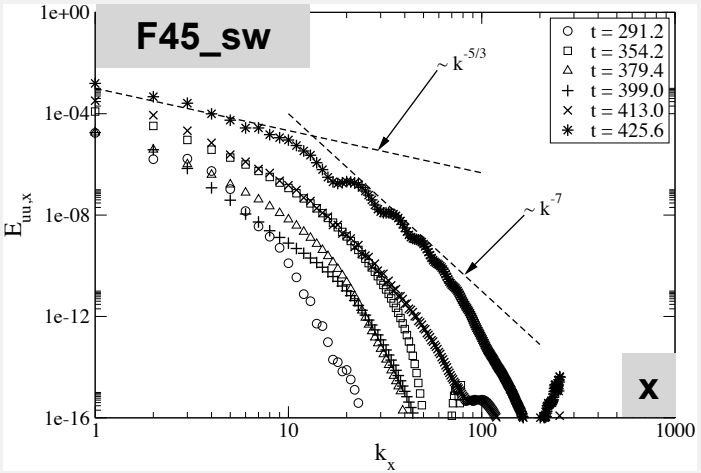
porous wall does not only delay transition/ transition onset it also alters the mode evolution

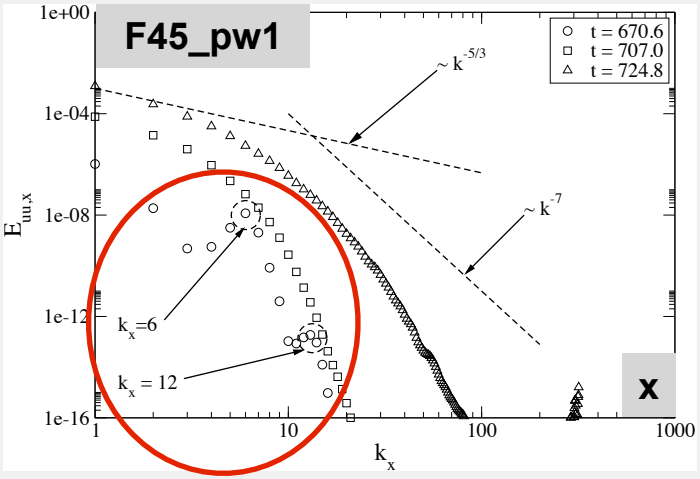


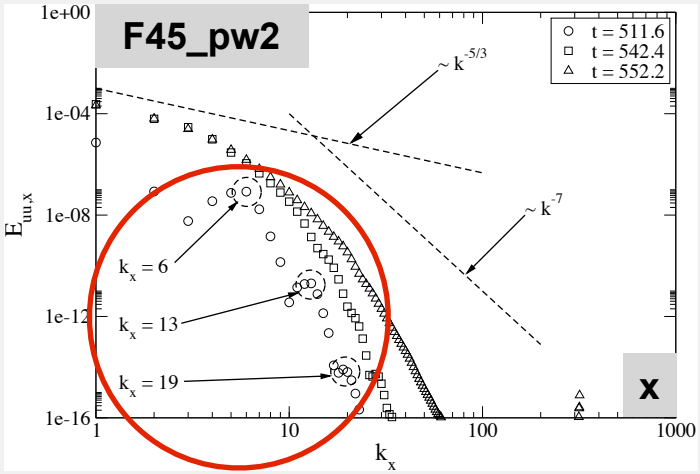


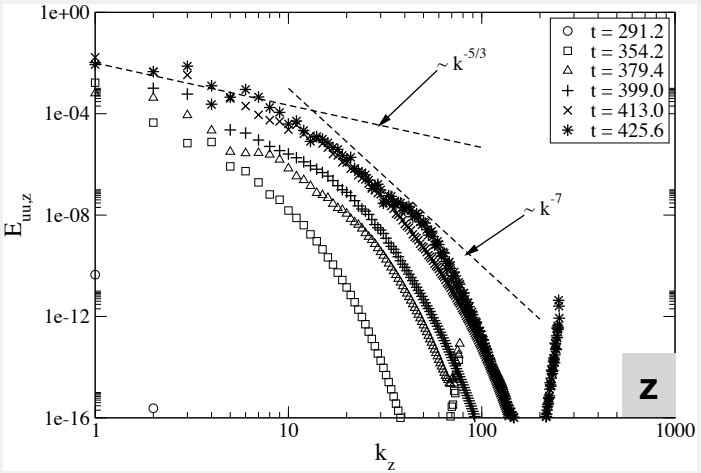
Energy Spectra

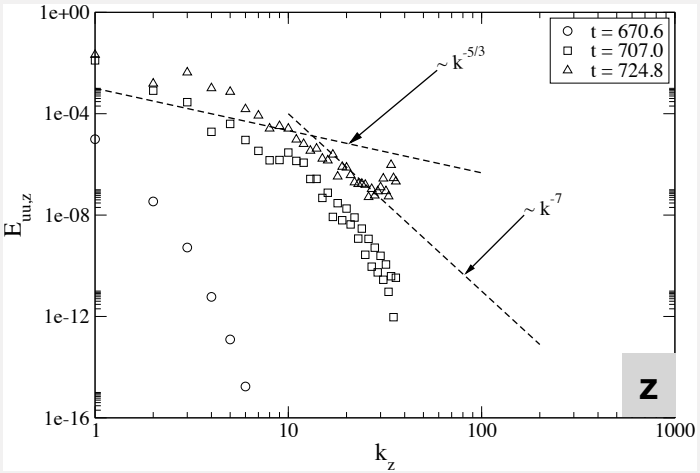
- power spectra (extracted at y ≈ 1) show that modes for porous wall cases contain significantly less energy in x compared to smooth wall cases although extracted at much later time
- harmonics appear in porous wall spectra which are not observed in smooth wall case

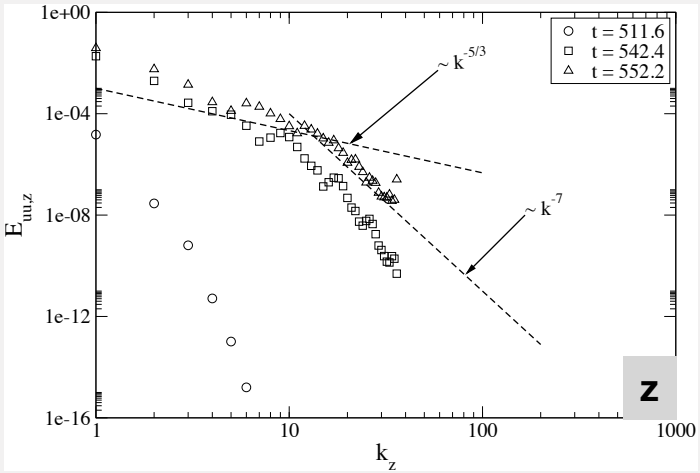








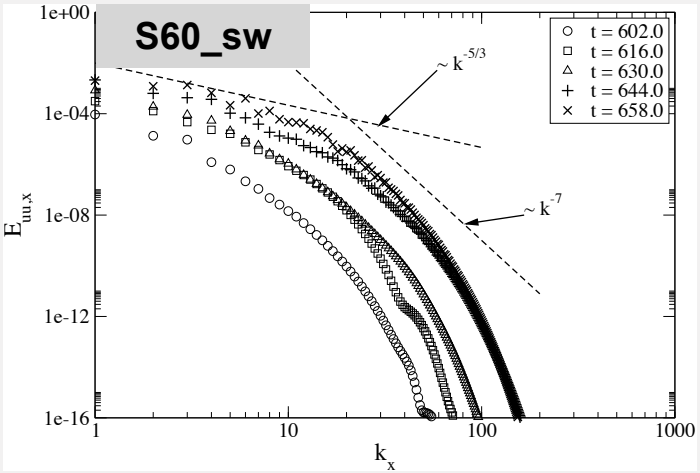


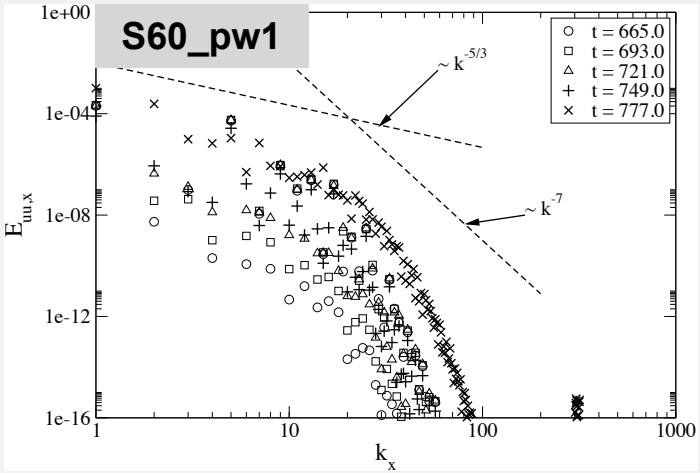


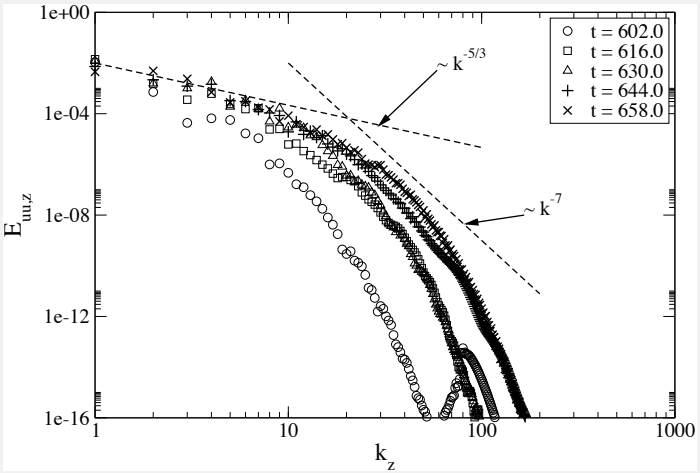
Energy Spectra

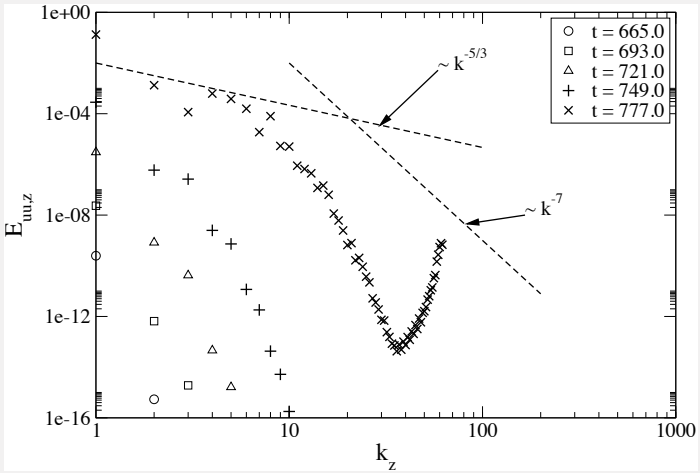
- similar to fundamental resonance
- modes in x and z have significantly less energy although extracted at much later times
- harmonics as seen in fundamental resonance case could not be observed

porous wall changes energy distribution among modes



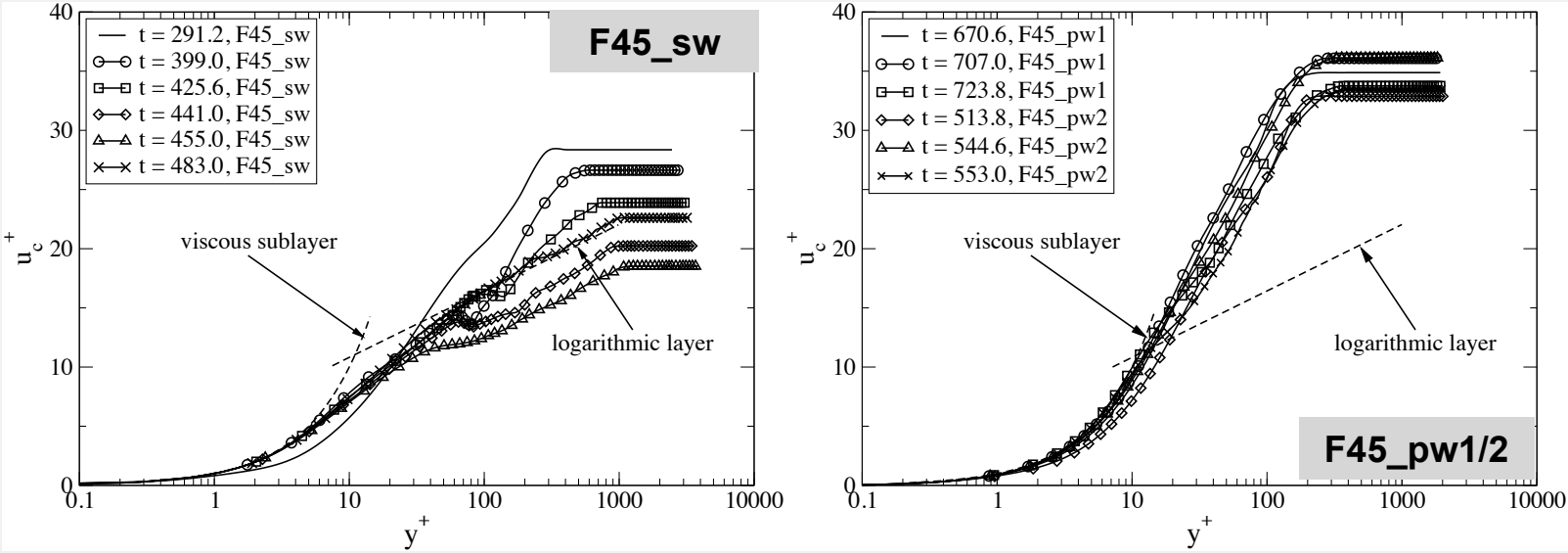






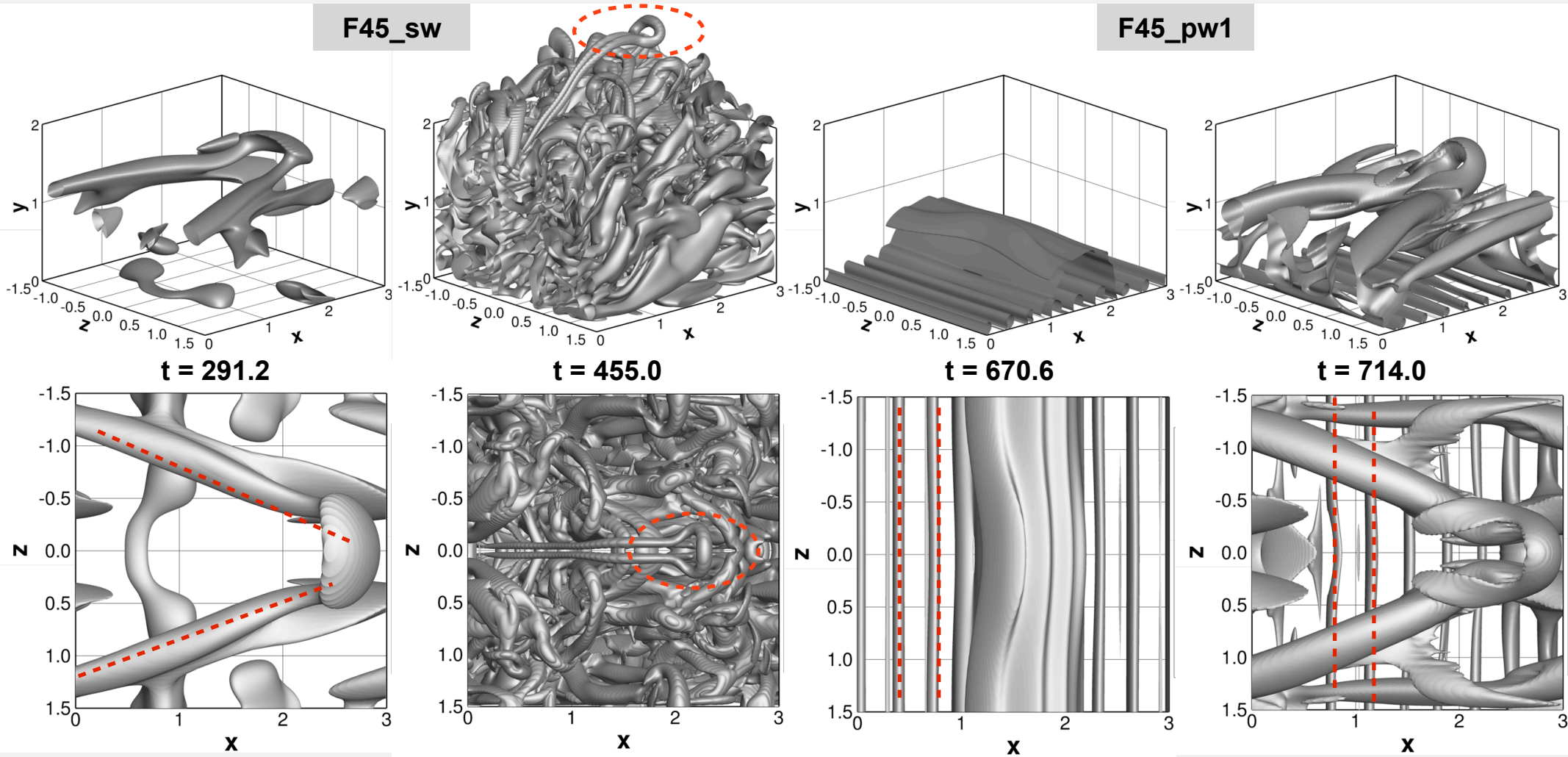
Van Driest Transformed Profiles

- breakdown process is significantly delayed by porous walls
- log layer develops much later or is not even observable for porous wall cases compared to smooth wall
- breakdown occurs much more rapidly for subharmonic case



Flow Structures (fundamental)

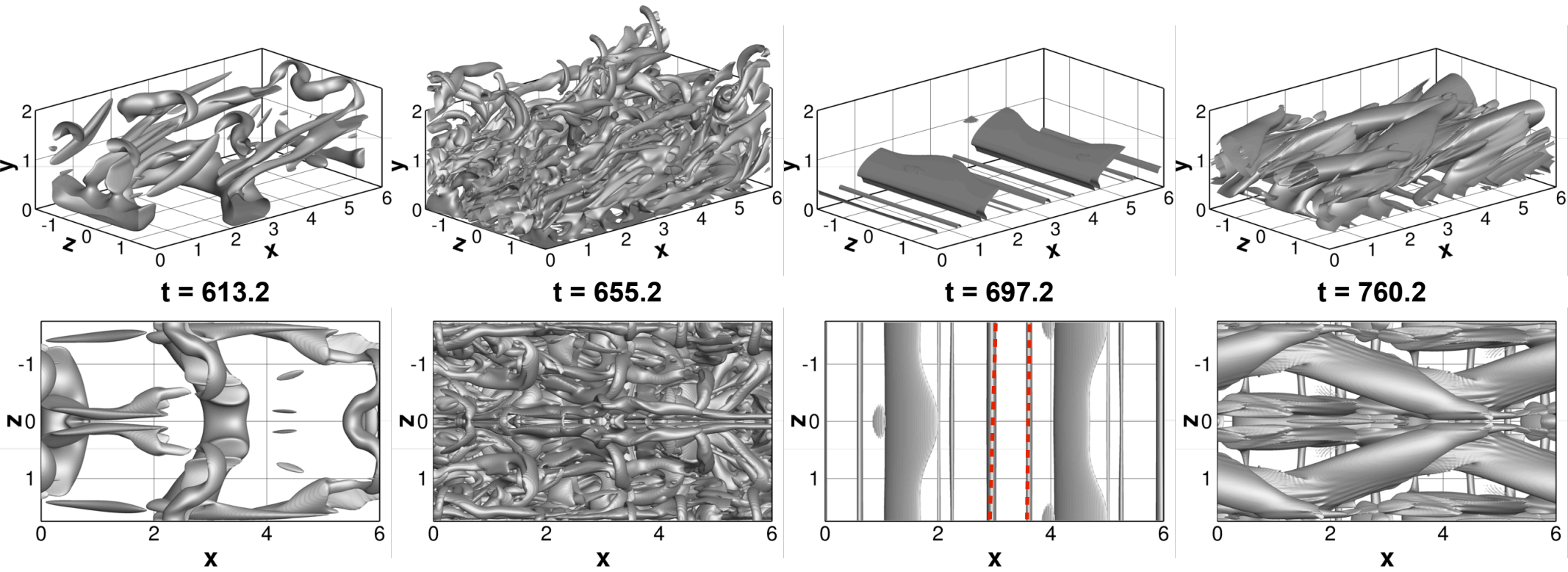
- **smooth wall:** typical formation of Λ-vortices and hairpin vortices, breakdown to small scales
- **porous wall:** development of Λ-vortices massively delayed, spanwise rollers at cavities



Flow Structures (subharmonic)

- **smooth wall:** typical staggered vortical patterns form, breakdown to small scales
- **porous wall:** spanwise vortices at the top of the cavities, predominantly two dimensional structures, breakdown to smaller scales occurs at a much later time

S60_sw **S60_pw1**



Outline



Introduction/Motivation

Governing Equations and Numerical Methods

Base Flow and Disturbance Generation

Linear Regime

Nonlinear Regime

Summary

Final Summary (1/2)



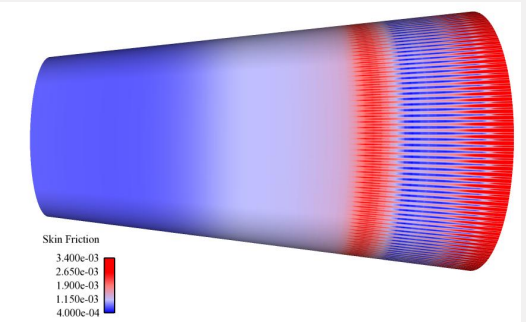
- higher-order immersed boundary method successfully applied to (nonlinear) transition simulations
- performed nonlinear simulations of smooth and porous wall geometry for fundamental and subharmonic breakdown scenario
- transition onset delayed for both scenarios in presence of porous wall
- porous wall significantly changes mode evolution, energy redistribution and as a consequence the evolution of vortical structures
- spanwise vortices observed at top of cavities

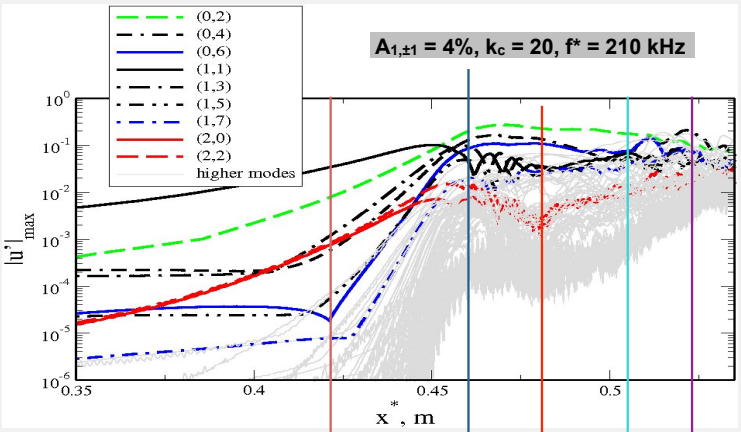
Final Summary (2/2)

Future work/suggested improvements:

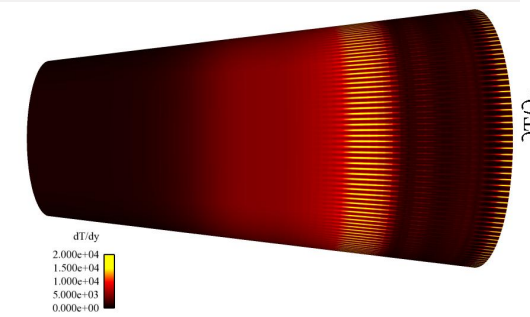
- apply immersed boundary to compute influence of roughness elements on transition on a cone (M = 6)
- Using 2D and 3D roughness for 'tailoring' the nonlinear breakdown process: Promising due to the stabilizing effects of compressibility on secondary instabilities
- include high temperature effects (non-constant c_p)
- run porous wall cases further into turbulence
- use more realistic flight conditions (isothermal wall/hot gas)

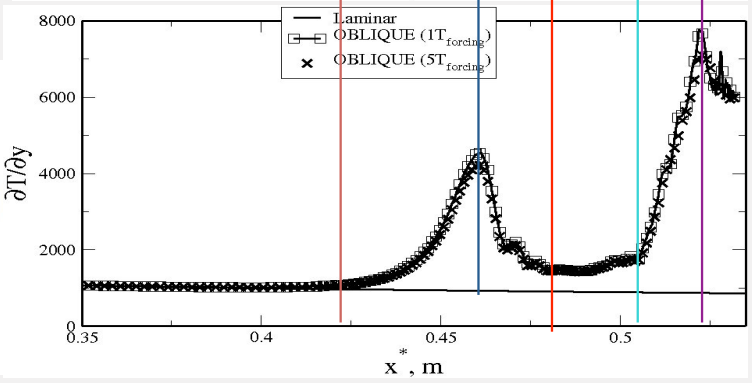
surface wall shear





surface heat flux







Thank you for your attention!